OXI1 and DAD Regulate Light-Induced Cell Death Antagonistically through Jasmonate and Salicylate Levels[1]

Inès Beaugelin,[a] Anne Chevalier,[a] Stefano D'Alessandro,[a] Brigitte Ksas,[a] Ondřej Novák,[b] Miroslav Strnad,[b] Céline Forzani,[c] Heribert Hirt,[d] Michel Havaux,[a,2,3] and Fabien Monnet[a,e]

[a]Aix-Marseille University, Centre National de la Recherche Scientifique, Commissariat à l'Energie Atomique et aux Energies Alternatives, UMR 7265 Biosciences and Biotechnologies Institute of Aix- Marseille, CEA/ Cadarache, F-13108 Saint-Paul-lès-Durance, France

[b]Laboratory of Growth Regulators, Institute of Experimental Botany, The Czech Academy of Sciences, Palacký University, CZ-78371 Olomouc, Czech Republic

[c]Institut Jean-Pierre Bourgin, Institut National de la Recherche Agronomique, AgroParisTech, Centre National de la Recherche Scientifique, Université Paris-Saclay, F-78000 Versailles, France

[d]Center for Desert Agriculture, King Abdullah University of Science and Technology, Thuwal, Saudi Arabia

[e]Université d'Avignon et des Pays de Vaucluse, F-84000 Avignon, France

ORCID IDs: 0000-0001-7618-9047 (I.B.); 0000-0002-0464-5549 (S.D.); 0000-0002-5369-3176 (B.K.); 0000-0002-2806-794X (M.S.); 0000-0003-3119-9633 (H.H.); 0000-0002-6434-393X (M.H.).

Singlet oxygen produced from triplet excited chlorophylls in photosynthesis is a signal molecule that can induce programmed cell death (PCD) through the action of the OXIDATIVE STRESS INDUCIBLE 1 (OXI1) kinase. Here, we identify two negative regulators of light-induced PCD that modulate *OXI1* expression: DAD1 and DAD2, homologs of the human antiapoptotic protein DEFENDER AGAINST CELL DEATH. Overexpressing *OXI1* in Arabidopsis (*Arabidopsis thaliana*) increased plant sensitivity to high light and induced early senescence of mature leaves. Both phenomena rely on a marked accumulation of jasmonate and salicylate. *DAD1* or *DAD2* overexpression decreased *OXI1* expression, jasmonate levels, and sensitivity to photooxidative stress. Knock-out mutants of *DAD1* or *DAD2* exhibited the opposite responses. Exogenous applications of jasmonate upregulated salicylate biosynthesis genes and caused leaf damage in wild-type plants but not in the salicylate biosynthesis mutant *Salicylic acid induction-deficient2*, indicating that salicylate plays a crucial role in PCD downstream of jasmonate. Treating plants with salicylate upregulated the *DAD* genes and downregulated *OXI1*. We conclude that OXI1 and DAD are antagonistic regulators of cell death through modulating jasmonate and salicylate levels. High light-induced PCD thus results from a tight control of the relative activities of these regulating proteins, with DAD exerting a negative feedback control on *OXI1* expression.

Cell death is essential for development and stress responses in all organisms (Greenberg, 1996; Kabbage et al., 2017). In contrast to necrosis, which involves uncontrolled cell lysis and fluid leakage, programmed cell death (PCD) is based on finely regulated genetic signaling. PCD has been widely studied in animals as apoptotic cell death, whereas it is relatively poorly documented in plants. At the cell scale, common features have been observed such as protease activation and DNA laddering, but few parallels have been found in terms of mechanisms.

Two main strategies have been undertaken to characterize PCD in plant cells. The first one focuses on phenotypic studies of the so-called lesion mimic mutants, allowing the identification of several genes involved in PCD in plants (Bruggeman et al., 2015). Different mechanisms can be affected in those mutants, including chloroplast metabolism, lipid synthesis and metabolism, membrane trafficking, secondary messenger signaling, such as by ion fluxes and reactive oxygen species (ROS), and control of gene expression. Actually, most studies on PCD highlight the central role

[1]This work was supported by the French National Research Agency (Agence Nationale de la Recherche project Signaling of Light-Induced Oxidative Stress in the Acclimation Mechanisms of Plants to Climatic Change [SLOSAM], 14-CE02-0010-02). I.B. was a recipient of a CEA-Irtelis PhD fellowship. O.N and M.S. are supported by a grant from the Ministry of Education, Youth and Sports of the Czech Republic (European Regional Development Fund-Project "Plants as a tool for sustainable global development" no. CZ.02.1.01/0.0/0.0/16_019/0000827) and the Czech Foundation Agency (grant no. 18-07563S).

[2]Author for contact: michel.havaux@cea.fr

[3]Senior author

The author responsible for distribution of materials integral to the findings presented in this article in accordance with the policy described in the Instructions for Authors (www.plantphysiol.org) is: Michel Havaux (michel.havaux@cea.fr).

M.H. initiated the study and secured the funding; I.B., M.H., and F.M. designed the experiments; I.B., A.C., S.D., and B.K. performed most experiments; O.N. and M.S. performed phytohormone analyses; C.F. and H.H. produced the OXI1-overexpressing Arabidopsis lines; I.B., S.D., M.H., F.M. analyzed the data; M.H. and I.B. wrote the article with input from the other authors.

www.plantphysiol.org/cgi/doi/10.1104/pp.19.00353

of ROS, primarily described as toxic compounds but which can also act as signaling molecules (Apel and Hirt, 2004; Van Breusegem and Dat, 2006; Khanna-Chopra et al., 2013; Petrov et al., 2015; Leister, 2019). ROS can be produced in different organelles, enabling the set-up of various signaling cascades leading either to acclimation or to cell death in specific environmental conditions (Gill and Tuteja, 2010). Mitochondria and chloroplasts are the energy factories of the plant cell, in which ROS are inevitable by-products of bioenergetic processes involving electron transport. ROS-mediated mitochondrial retrograde signaling leading to cell death has been observed especially during UV-induced plant PCD (Gao et al., 2008). Within chloroplasts, the electron transfer chain and triplet state excited chlorophylls are major sites of ROS production. One of the first studies establishing a role for the chloroplast in the signaling of PCD showed that the expression of anti-apoptotic proteins of the mammalian B-cell lymphoma-2 (Bcl-2) family in chloroplasts suppressed light-driven apoptotic-like lesions induced by chloroplast-directed herbicides (Chen and Dickman, 2004).

The Arabidopsis (*Arabidopsis thaliana*) *fluorescent in blue light* mutant (*flu*) is one of the lesion mimic mutants; it accumulates a chlorophyll precursor in the dark and consequently produces high amounts of singlet oxygen ($^1O_2$), leading to cell death, after transfer from darkness to light (Meskauskiene et al., 2001; op den Camp et al., 2003). A suppressor screen in the *flu* mutant background led to the identification of the first mediators of $^1O_2$-induced cell death, the plastid proteins EXECUTER1 and EXECUTER2 (Wagner et al., 2004; Kim et al., 2012). Since the pioneer studies on *flu*, $^1O_2$ signaling leading to PCD has been widely studied and extended to other Arabidopsis mutants, such as the chlorophyll b-deficient *chlorina 1* (*ch1*) mutant that overproduces $^1O_2$ from the PSII reaction centers (Ramel et al., 2013a). ROS-mediated signaling is known to involve phytohormones, especially jasmonate, salicylate, and abscisic acid (Noctor et al., 2015), and phytohormones have an important regulatory function in PCD in both *flu* and *ch1* (Laloi and Havaux, 2015). In particular, jasmonate accumulation sets the threshold between acclimation and cell death during high light stress (Ramel et al., 2013b; Shumbe et al., 2016). High-light jasmonate-driven PCD involves the OXIDATIVE STRESS INDUCIBLE 1 (OXI1) kinase through a new mechanism, apparently independent from its role in plant-pathogen interactions (Rentel et al., 2004), since it does not involve induction of the mitogen-activated protein kinases (MPKs) 3 and 6 (Shumbe et al., 2016). OXI1 (also called AGC2-1) is a membrane protein of the AGC kinase family that is present in all plant organs and is mainly localized at the cell periphery (Anthony et al., 2004). The knock-out (KO) mutant of *OXI1* displays a phenotype with increased resistance to high light, which is associated with reduced accumulation of jasmonate (Shumbe et al., 2016)

The second strategy in investigating PCD in plants consists of searching for orthologous proteins of apoptotic effectors. Caspase proteins are the main mammalian cell death effectors, but no orthologs have been found in plants. However, proteins with caspase-like activity have been described in plants by their response to chemical caspase-3 inhibitors, showing that plants and animals share an ancestral common PCD pathway (Ge et al., 2016). As mentioned above, transgenic tobacco lines (*Nicotiana tabacum*) expressing members of the mammalian Bcl-2 protein family avoided PCD induced by herbicides (Chen and Dickman, 2004), showing that mammalian antiapoptosis effectors can modulate plant PCD. Moreover, Bax inhibitor (BI) has homologs in animals, yeast, and plants. In particular, AtBI1 has been reported as an inhibitor of hydrogen peroxide-, salicylic acid-, heat-, and cold-induced cell death in plants (Kawai-Yamada et al., 2004; Nagano et al., 2009).

Another homologous protein found in both animal and plant cells is DEFENDER AGAINST CELL DEATH 1 (DAD1). Its function as a PCD inhibitor is conserved among species, since complementation by the Arabidopsis *AtDAD1* rescues animal cells from apoptosis (Gallois et al., 1997). The over-expression of *AtDAD1* and *AtDAD2* (a second Arabidopsis homolog) in protoplasts rescues cells from UV-induced PCD (Danon et al., 2004). Interestingly, transcriptomic analyses of the $^1O_2$-producing *ch1* mutant showed that expression of *DAD1* was induced under acclimatory light conditions rather than under conditions leading to PCD, suggesting a possible protective role against $^1O_2$-induced cell death (Ramel et al., 2013a).

In this work, we used *OXI1*, *DAD1*, and *DAD2* inactivation and overexpression to investigate high light-induced PCD in Arabidopsis and its regulation by phytohormones. The present data identify the DAD proteins as negative regulators of PCD. They also reveal a complex interplay of the antagonistic actions of OXI1, DAD1, and DAD2 on jasmonate and salicylate levels, determining the orientation of plant responses toward cell death or photoacclimation.

RESULTS

High *OXI1* Expression Levels Accelerate Senescence and Exacerbate High-Light-Induced Cell Death

Among several homozygous *OXI1*-overexpressing (OE:OXI1) lines, lines 35 and 8054 were chosen for their strong expression of *OXI1*, while line 8053 exhibited a weaker expression (Fig. 1A). During the first 4 weeks of growth in short-day conditions (8-h light), high expression levels of *OXI1* had no visible effect on the plant phenotype: growth rate (Fig. 1B) and plant morphology (Fig. 1C) did not differ between wild-type and OE:OXI1 plants. However, growth of the stronger overexpressors (lines 35 and 8054) virtually stopped at week 5 (Fig. 1B). This growth arrest was accompanied by a yellowing of the older leaves, which subsequently died (Fig. 1C), and was present in 100% of the

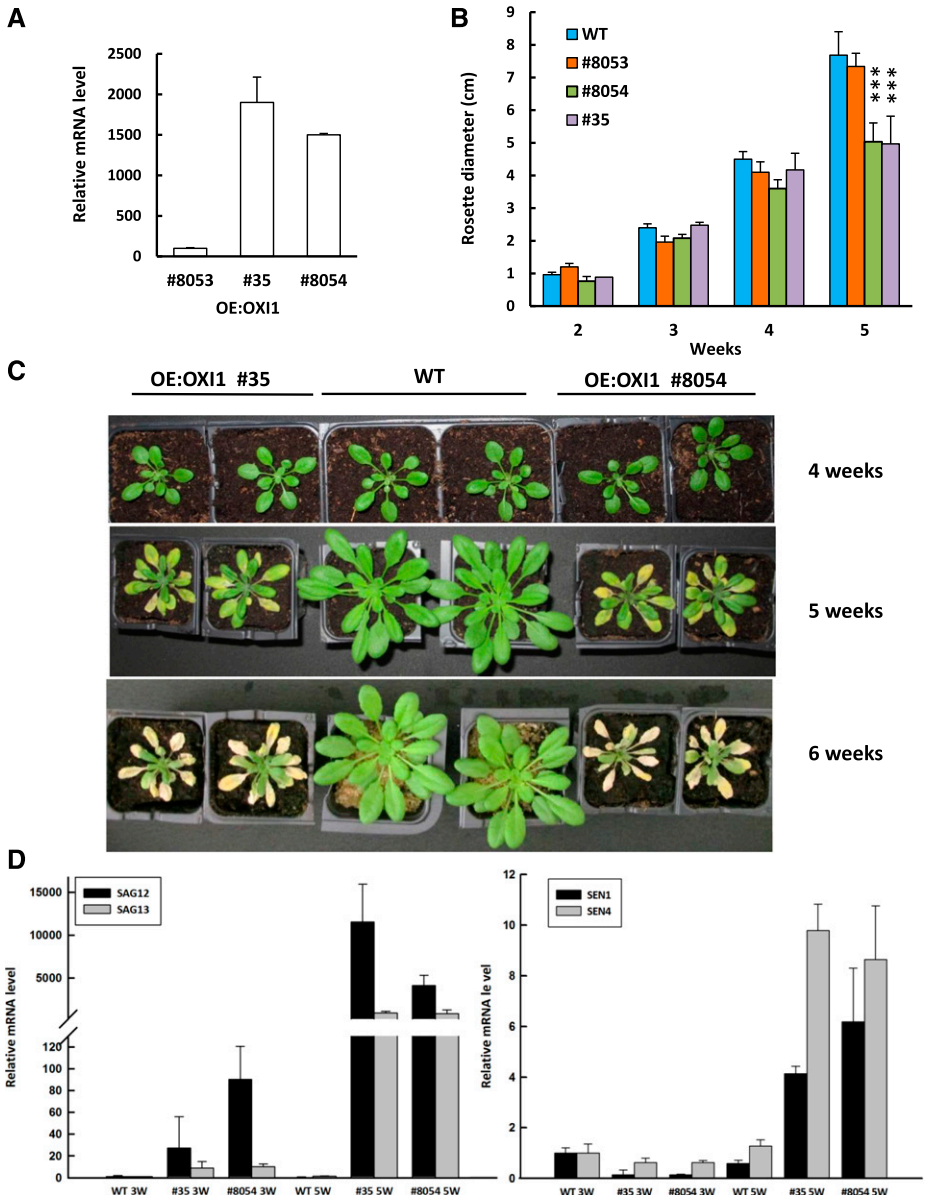

Figure 1. Overexpressing *OXI1* in Arabidopsis leads to an accelerated senescence phenotype. A, RT-qPCR analysis of the expression levels of *OXI1* in three OE:OXI1 lines (35, 8053, and 8054) relative to the wild type. $n = 3$ biological replicates. B, Growth curves of wild-type plants and the three OE:OXI1 lines ($n = 3$). Plants were grown under short-day conditions (photoperiod, 8 h). $^{***}P < 0.001$ compared to the wild type, as determined by Student's t test. C, Phenotype of wild-type and OE:OXI1 plants at different ages (4, 5, and 6 weeks). D, Senescence marker genes *SAG12*, *SAG13*, *SEN1*, and *SEN4* in leaves of wild type and OE:OXI1 lines 35 and 8054 aged 3 weeks and 5 weeks (3W and 5W, respectively). RT-qPCR measured expression levels are normalized to the wild-type levels at week 3 ($n = 3$).

transgenic plants. In contrast, these phenomena were absent in the milder line (8053) and in the *oxi1* KO mutant, as previously shown (Shumbe et al., 2016). Furthermore, the senescence phenotype of the OE:OXI1 plants seemed to be light dependent, since it was amplified in plants grown at a photon flux density (PFD) of 130 μmol photons m^{-2} s^{-1} compared to plants grown at 90 μmol m^{-2} s^{-1} (Supplemental Fig. S1).

The phenotype of 5-week-old OE:OXI1 plants (Fig. 1C) suggests that high *OXI1* expression levels lead to accelerated senescence and PCD. This hypothesis was confirmed in Figure 1D by the analysis of the senescence marker genes *SENESCENCE ASSOCIATED GENE12* (*SAG12*), *SAG13*, *SENESCENCE1* (SEN1), and *SEN4* (Lohman et al., 1994; Oh et al., 1996; Gan and Amasino, 1997; Qi et al., 2015) in plants aged 3 and 5 weeks. In the wild type, the expression level of those genes was low and did not change significantly from week 3 to week 5. In striking contrast, there was a marked increase in the transcripts of the four genes in the OE:OXI1 lines 35 and 8054 at 5 weeks, indicating the establishment of an early senescence mechanism.

When 4-week-old plants were exposed for 1 d to photooxidative stress (1,500 μmol photons m^{-2} s^{-1} at 7°C), considerable oxidative damage was observed in the OE:OXI1 lines as indicated by the bleaching of most of the leaves (Fig. 2A). This was accompanied by lipid peroxidation, as shown by autoluminescence imaging (Fig. 2B), and hydroxy-octadecatrienoic acid (HOTE) quantification (Fig. 2D). Plant autoluminescence is indicative of lipid peroxide accumulation, the slow decomposition of which is associated with photon emission (Birtic et al., 2011), and HOTEs are oxidation products of linolenic acid (C18:3), the major

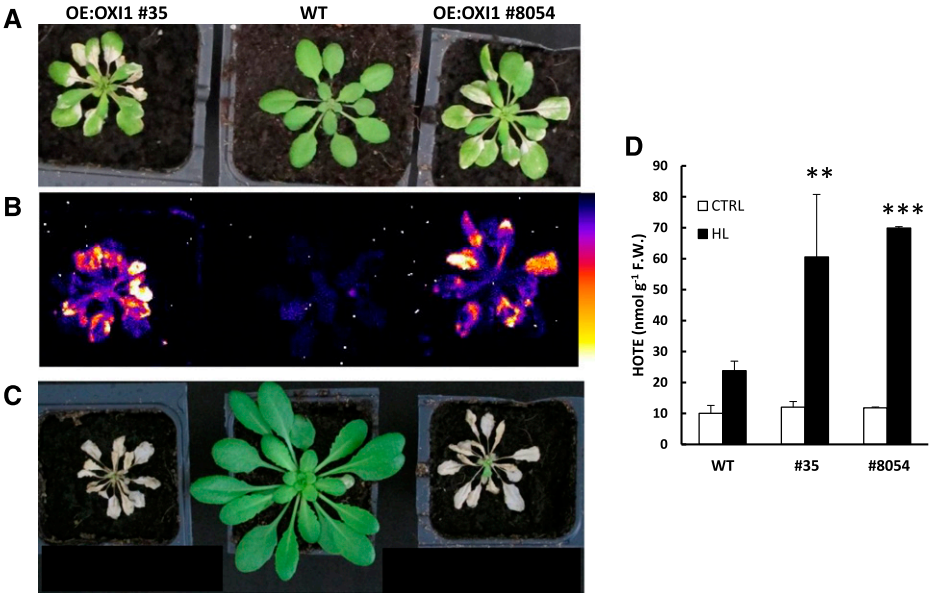

Figure 2. Overexpressing *OXI1* in Arabidopsis decreases tolerance to photooxidative damage. A, Picture of wild-type and OE:OXI1 plants aged 3 weeks after exposure to high light stress (1 d at 1,500 μmol photons m^{-2} s^{-1} at 7°C). B, Lipid peroxidation visualized by autoluminescence imaging. The color palette indicates luminescence intensity from low (dark blue) to high values (white). C, Picture of the high light-treated plants after transfer to normal growth conditions (8 d in the phytotron after stress). D, HOTE levels before (CTRL) and after high light (HL) stress ($n = 3$). F.W., fresh weight. $^{**}P < 0.01$ and $^{***}P < 0.001$, compared with wild type (Student's *t* test).

polyunsaturated fatty acid in plant leaves (Montillet et al., 2004). These phenomena were not observed in wild-type plants or the OE:OXI1 line 8053. When plants were transferred back to standard growth conditions in the phytotron, wild-type plants continued to grow, whereas OE:OXI1 plants died (Fig. 2C). The response of the OE:OXI1 plants is thus opposite that of the *oxi1* mutant, which was reported to be noticeably less sensitive than the wild type to high light-induced cell death (Shumbe et al., 2016).

Hormonal Changes Associated with *OXI1* Expression and Cell Death

The phytohormone jasmonate is essential for $^1O_2$-induced PCD (Ramel et al., 2013a), and OXI1 has been proposed to regulate PCD by modulating jasmonate levels (Shumbe et al., 2016). Accordingly, in the *oxi1* null mutant that is resistant to light-induced PCD, jasmonate content in leaves is substantially reduced compared to that in the wild type (Shumbe et al., 2016). This was confirmed in our study, as shown in Figure 3A, which shows a reduction of jasmonate content by ~50% in *oxi1* relative to the wild type both under control conditions and after high light stress. Interestingly, salicylic acid content was also affected by the *oxi1* mutation, with the biosynthesis of this phytohormone being almost completely blocked in the *oxi1* mutant (Fig. 3D).

The opposite behavior was observed in OE:OXI1 plants, with jasmonate content increasing by a factor of approximately two compared to that in the wild type. *OXI1* overexpression had the same effect on the content of the jasmonate active form, jasmonoyl-Ile (Fig. 3B), and the jasmonate precursor cis-12-oxo-phytodienoic acid (OPDA; Fig. 3C), indicating a stimulation of the whole jasmonate biosynthesis pathway when *OXI1* expression was high. This was confirmed by reverse transcription quantitative PCR (RT-qPCR) analysis of the expression of the jasmonate biosynthesis genes *LIPOXYGENASE2* (*LOX2*) and *OXOPHYTODIENOATE REDUCTASE3* (*OPR3*): both genes were strongly induced in OE:OXI1 plants compared to wild-type plants (Fig. 3, E and F). Salicylic acid showed a similar (and amplified) response to the enhancement of *OXI1* expression, with a considerable increase (10-fold or more) in salicylic acid concentration in OE:OXI1 leaves relative to wild-type leaves, both in low light and in high light (Fig. 3D). Salicylic a cid concentration in Arabidopsis leaves thus appears to be highly responsive to OXI1 abundance. Accordingly, the *ENHANCED DISEASE SUSCEPTIBILITY1* (*EDS1*) gene involved in salicylate biosynthesis was strongly up-regulated in OE:OXI1 plants (Fig. 3G). Moreover, the salicylate-responsive gene *PATHOGENESIS-RELATED GENE1* (*PR1*), a proxy of salicylate biosynthesis, exhibited a remarkable rise in expression (Fig. 3H).

To check for a causal link between the OXI1-mediated hormonal changes and cell death, *OE:OXI1* lines 35 and 8054 were crossed with the salicylic acid-deficient mutant *sid2* (Wildermuth et al., 2001; Fig. 4). The homozygous OE:OXI1 × *sid2* plants contained less salicylic acid than OE:OXI1 plants (Fig. 4C). The senescence-type phenotype observed in both OE:OXI1 lines was not observed in the OE:OXI1 × *sid2* plants (Fig. 4A). Thus, accumulation of salicylic acid was instrumental in the premature senescence and cell death phenomena observed in the OE:OXI1 lines. We also crossed the transgenic OE:OXI1 line 35 with the *delayed dehiscence2* (*dde2*) mutant, which is a null mutant for the *ALLENE OXIDE SYNTHASE* (*AOS*) gene and lacks jasmonate. The senescence and PCD observed in the OE:OXI1 plants was absent from the OE:OXI1 × *dde2* plants, confirming the involvement of jasmonate in those phenomena (Fig. 4B). Interestingly, the salicylate

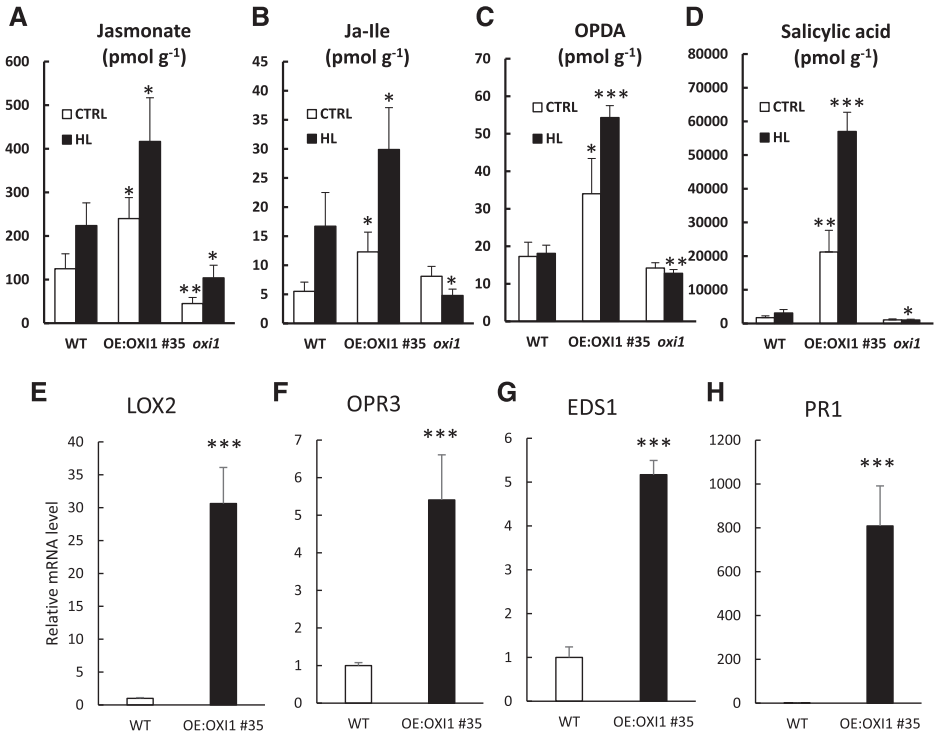

Figure 3. Overexpressing *OXI1* in Arabidopsis induces accumulation of jasmonate and salicylic acid. A to D, Hormone levels of jasmonate (A), jasmonoyl Ile (B), OPDA (C), and salicylic acid in pmol g^{-1} fresh weight (D) in the wild type, OE:OXI1 line 35, and the *oxi1* KO mutant before (CTRL) and after high light stress (HL; 2 d at 1,500 μmol m^{-2} s^{-1} at 7°C; $n = 5$). E and F, Expression levels of the jasmonate biosynthesis genes, *LOX2* and *OPR3*, in the wild type and OE:OXI1 (line 35). G and H, Expression levels of the salicylate biosynthesis genes, *EDS1* and *PR1*, in the wild type and OE:OXI1 (line 35). $^{*}P < 0.05$, $^{**}P < 0.01$, and $^{***}P < 0.001$, compared to the wild type (Student's *t* test).

content of OE:OXI1 × *dde2* leaves was close to that of wild-type leaves (Fig. 4D). As shown in Supplemental Figure S2A, the *dde2* and *sid2* mutations fully restored the growth of OE:OXI1 line 35. Finally, we analyzed the expression of jasmonate biosynthesis genes (*LOX2* and *OPR3*) in the OE:OXI1 × *sid2* plants compared to OE:OXI plants (Supplemental Fig. S2B). Both genes were noticeably induced in OE:OXI1 compared to the

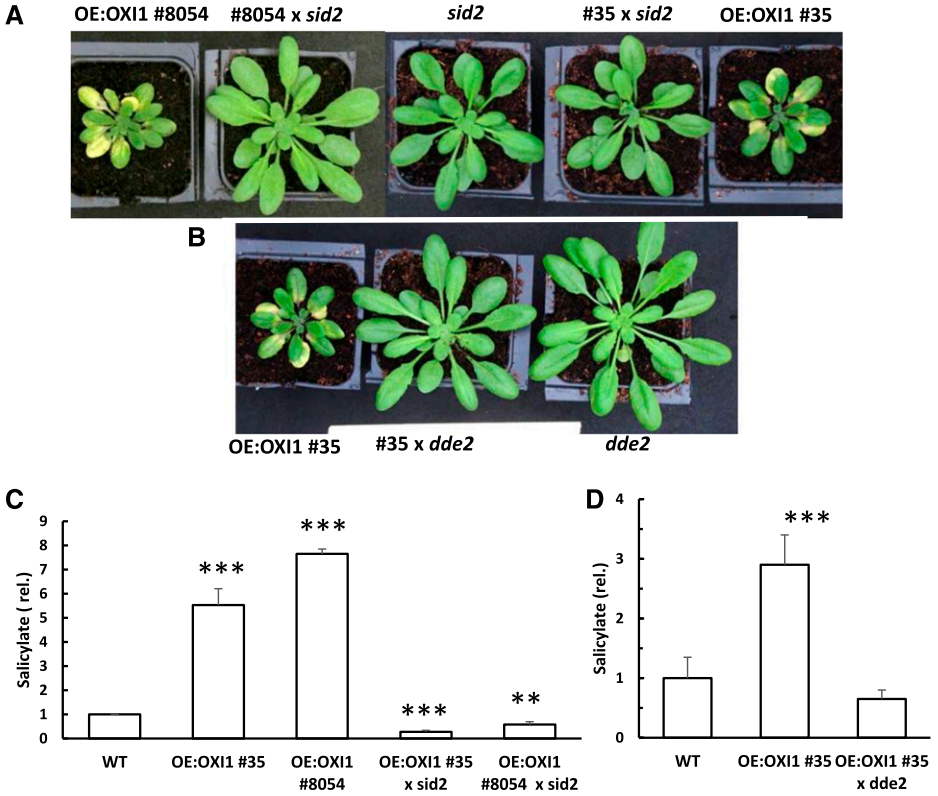

Figure 4. The senescence phenotype of the *OE:OXI1* plants (line 35) is dependent on the accumulation of jasmonate and salicylic acid. A and B, Pictures of 5-week-old OE:OXI1 plants with reduced salicylic acid synthesis or jasmonate synthesis due to *sid2* (A) or *dde2* (B) mutations, respectively. The single mutants *sid2* and *dde2* are also shown for comparison purposes. C and D, Salicylate levels ($n = 3$). $^{**}P < 0.01$ and $^{***}P < 0.001$, compared with the wild type (WT; Student's *t* test). Rel = relative to wild type level.

wild type (Fig. 3). *LOX2* and *OPR3* remained induced in OE:OXI1 × *sid2* plants. Thus, the *sid2* mutation appeared to have limited effects on the expression levels of jasmonate biosynthesis-related genes in the OXI1 enriched background.

OXI1 has been previously shown to link oxidative burst signals during pathogen-plant interactions and downstream responses through activation of MPKs, especially MPK3 and MPK6 (Rentel et al., 2004). *MPK3* and *MPK6* expression was analyzed in the OE:OXI1 plants, and no significant difference from the wild type was observed (Supplemental Fig. S3).

Four-week-old OE:OXI1 (line 35) plants and OE:OXI1 × *dde2* and OE:OXI1 x *sid2* mutant plants were exposed to high light stress (Fig. 5). As previously shown in Figure 2, this treatment induced extensive oxidative damage to OE:OXI1 leaves. In striking contrast, both double mutants were resistant to high light, as shown by their strongly diminished autoluminescence intensity and HOTE levels compared to OE:OXI1. This finding confirms the involvement of jasmonate and salicylate in photosensitivity associated with *OXI1* overexpression.

DAD1 and *DAD2* Expression Is Modified by High Light and by *OXI1* Overexpression

A previous transcriptomic study of the $^1O_2$-overproducing mutant *ch1* (Ramel et al., 2013a) pointed to another potentially interesting gene that encodes a protein homologous to the human antiapoptotic protein DAD1 (Yulug et al., 1995). The animal DAD1 protein is an integral membrane protein that resides in the endoplasmic reticulum (ER; Makishima et al., 1997), and this localization was confirmed in plants (Danon et al., 2004). In contrast with *OXI1* expression, which was induced by light conditions leading to cell death (Shumbe et al., 2016), *DAD1* expression was especially induced by acclimatory light conditions that lead to increased tolerance to photooxidative stress (Ramel et al., 2013a). This effect was confirmed here by RT-qPCR (Fig. 6A) and is consistent with the known function of DAD1 in animals and humans.

The Arabidopsis genome shows two genes coding for DAD proteins: *DAD1* and *DAD2*. The coding sequences of the two *DAD* genes are 95.7% identical (Danon et al., 2004). They share the same organization, with variations only in intron sizes. However, the regulation of *DAD1* appears to be different from that of *DAD2*, since *DAD2* was more highly induced by light conditions leading to cell death than by acclimation conditions (Fig. 6A). In addition, *DAD1* expression was enhanced in OE:OXI1 line 35 compared to the wild type, while the effect on *DAD2* expression was less pronounced (Fig. 6B).

DAD1 and DAD2 Are Negative Regulators of High Light-Induced Cell Death

The *dad1* and *dad2* mutants deficient in DAD1 or DAD2, respectively, were both null mutants for the respective *DAD* transcript (Fig. 7A). Suppression of *DAD1* had no significant impact on the expression of the *DAD2* gene while suppression of *DAD2* led to a repression of the *DAD1* gene (Fig. 7B). These results do not support a compensatory effect on the expression of one *DAD* gene in the absence of the other.

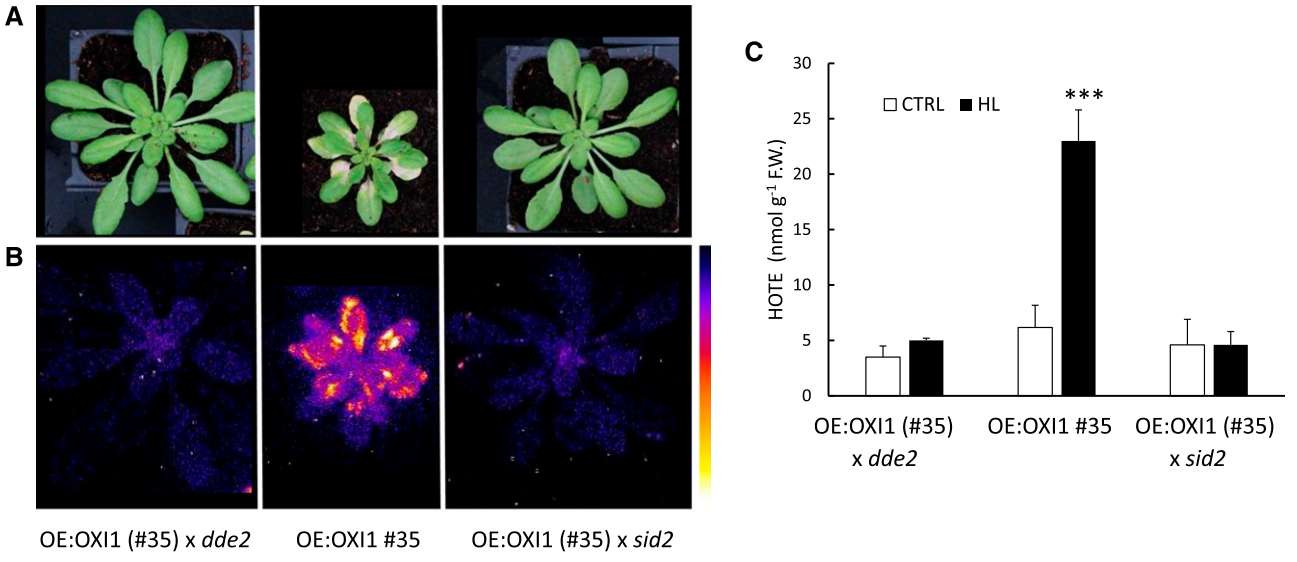

Figure 5. The photosensitivity of *OE:OXI1* plants depends on jasmonate and salicylate levels. A, Pictures of plants aged 3 weeks (OE:OXI1 line 35, OE:OXI1 × *dd2*, and OE:OXI1 × *sid2*) after exposure to high light stress (1 d at 1,500 μmol photons m^{-2} s^{-1} at 7°C). B, Lipid peroxidation visualized by autoluminescence imaging. The color palette indicates luminescence intensity from low (dark blue) to high values (white). C, HOTE levels before (CTRL) and after high light (HL) stress ($n = 3$). F.W., fresh weight. ***$P <$ 0.001, compared to the control condition (Student's *t* test).

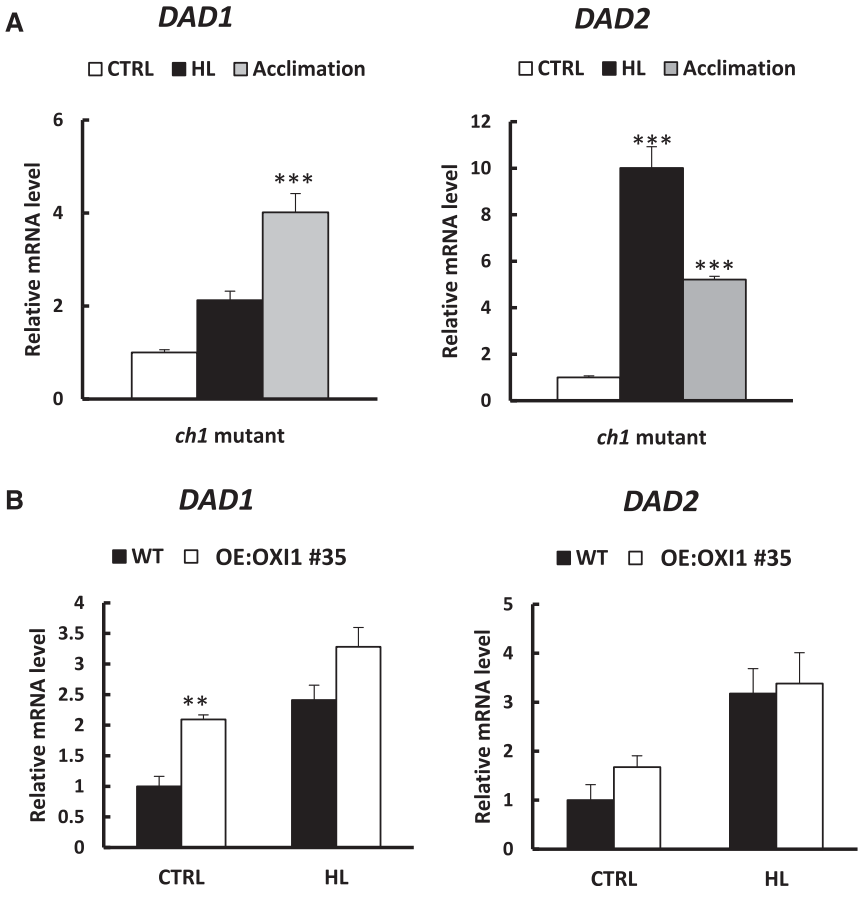

Figure 6. RT-qPCR analysis of *DAD1* and *DAD2* expression in leaves of wild-type (WT) Arabidopsis, the *ch1* mutant, and OE:OXI1 line 35. A, *DAD1* and *DAD2* expression levels in leaves of the *ch1* mutant in control (CTRL), high light (HL) stress, and acclimation conditions ($n = 3$). HL = 1,200 μmol m^{-2} s^{-1} at 10°C for 8 h; acclimation = 450 μmol photons m^{-2} s^{-1} at 20°C for 48 h. B, *DAD1* and *DAD2* expression levels in leaves of the wild type and OE:OXI1 35 in control and high light stress conditions ($n = 3$). HL = 1,500 μmol photons m^{-2} s^{-1} at 8°C for 8 h. Data are expressed relative to wild-type or *ch1* levels in control conditions. $^{**}P < 0.01$ and $^{***}P < 0.001$, compared to CTRL (Student's *t* test).

When exposed to photooxidative stress conditions for 24 h, the *dad1* and *dad2* KO mutants showed more damage than the wild type (Fig. 7, C and D). To relate this observation with an induction of PCD, we analyzed the expression of several PCD marker genes (*N-rich protein1* [*NRP1*], *NRP2*, *VACUOLAR PROCESSING*

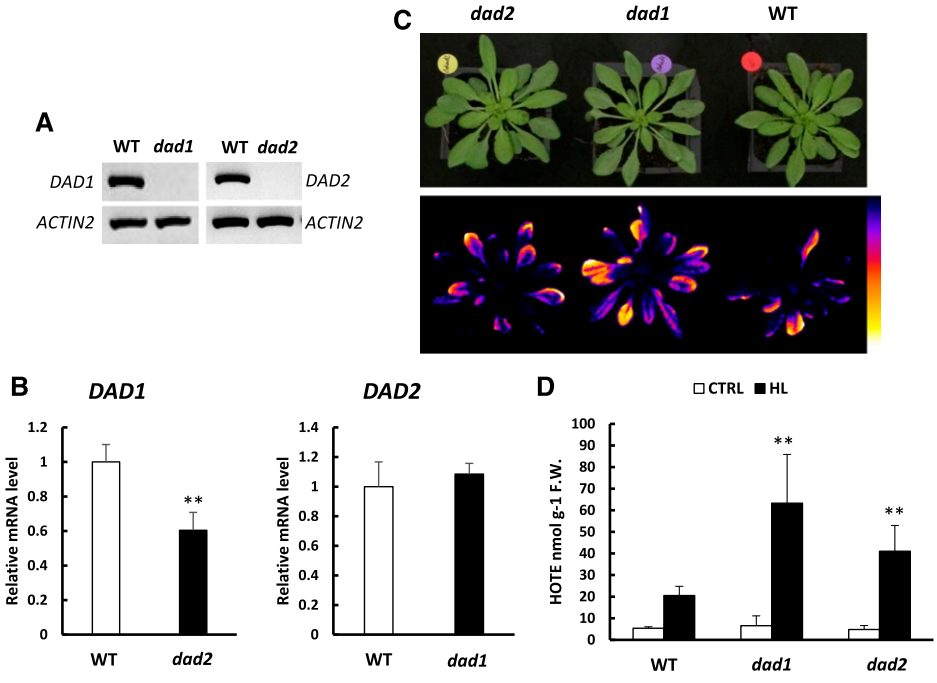

Figure 7. The *dad1* and *dad2* KO mutants exhibit an increased sensitivity to photooxidative damage. A, RT-PCR analysis of the KO mutation in the *dad1* and *dad2* mutants. *ACTIN2* was used as control. B, *DAD1* expression in the *dad2* mutant and vice versa ($n = 3$). C, Phenotype (top) and autoluminescence imaging (bottom) of the *dad1* and *dad2* KO mutants after 24 h in high light (HL) stress (1,500 μmol m^{-2} s^{-1} 7°C/18°C day/night). The experiment was stopped when symptoms of leaf damage and photooxidative stress were visible in the *dad* mutants (24 h treatment). The color palette indicates luminescence intensity from low (dark blue) to high values (white). D, HOTE levels before (CTRL) and after high light stress ($n = 5$). F.W., Fresh weight. $^{**}P < 0.05$ (C) and $^{**}P < 0.01$ (D), compared to the wild type (Student's *t* test).

ENZYME [*gVPE*], *Metacaspase 8* [*MC8*], *ARABIDOPSIS NAC DOMAIN CONTAINING PROTEIN089* [*ANAC089*], *EDS1*, and *Phytoalexin deficient 4* [*PAD4*]; Fig. 8). NRP1 and NRP2 are cell death mediators under ER and osmotic stress that activate an effector of the cell death response (Alves et al., 2011; Reis and Fontes, 2012; Reis et al., 2016). gVPE exhibits caspase-2-like activity and induces plant-specific PCD, modulating the collapse of the vacuole (Hatsugai et al., 2015; Petrov et al., 2015). MC8 is part of a PCD pathway activated by oxidative stress (He et al., 2008; Petrov et al., 2015). ANAC089 is up-regulated by ER stress and plays a role in regulating downstream genes involved in PCD (Yang et al., 2014; Petrov et al., 2015). Finally, EDS1 and PAD4 are recognized regulators of cell death, constituting a regulatory hub that transduces redox signals in response to biotic and abiotic stresses (Wituszynska and Karpinski, 2013; Petrov et al., 2015). High light induced expression of all the selected genes, but the effect was amplified in the *dad* mutants compared to the wild type (Fig. 8, A–G). In general, high light-induced gene expression was more pronounced in *dad2* compared to *dad1*. The results shown in Figure 8 show that high light induces PCD and confirm the inhibiting effects of DAD1 and DAD2 on PCD processes. These findings are confirmed by cell death evaluations using Trypan Blue staining (Fig. 8H). High light induced cell death, as shown by the increased blue coloration of the leaves. Trypan Blue staining was further increased in the *dad* mutants, indicating the presence of more dead cells compared to wild-type leaves. The effect was more pronounced in the *dad2* mutant compared to *dad1*. The up-regulation of several genes associated with ER-stress-induced PCD (*ANAC089*, *NRP*, and *VPE*) in the *dad* mutants is in line with the ER localization of DAD and suggests a role for the ER in response to high light stress. In contrast, homozygous overexpressor lines of *DAD1* (OE:DAD1) or *DAD2* (OE:DAD2; Fig. 9A) were all more resistant than the wild type to high light stress, as indicated by minor leaf bleaching (Fig. 9, B and D) and lipid peroxidation (Fig. 9, B–E) after 28 h exposure to photooxidative stress conditions. The duration of the stress treatments in Figures 8 and 9 were different, because in one case (comparison between *dad* KO mutants and the wild type), the purpose was to observe an increased photosensitivity of the *dad* mutants compared to the wild type, whereas in the other case (OE:DAD versus the wild type), a decreased sensitivity of the overexpressors was expected. Thus, the stress treatment was shorter in Figures 7 and 8 (24 h) compared to Figure 9 (28 h). Consequently, wild-type plants were more stressed in the latter experiments (Fig. 9), accumulating higher HOTE levels and showing more extended cell death compared to Figures 7 and 8. The extent of cell death was noticeably reduced in the DAD-overexpressing lines compared to the wild type. The responses of the

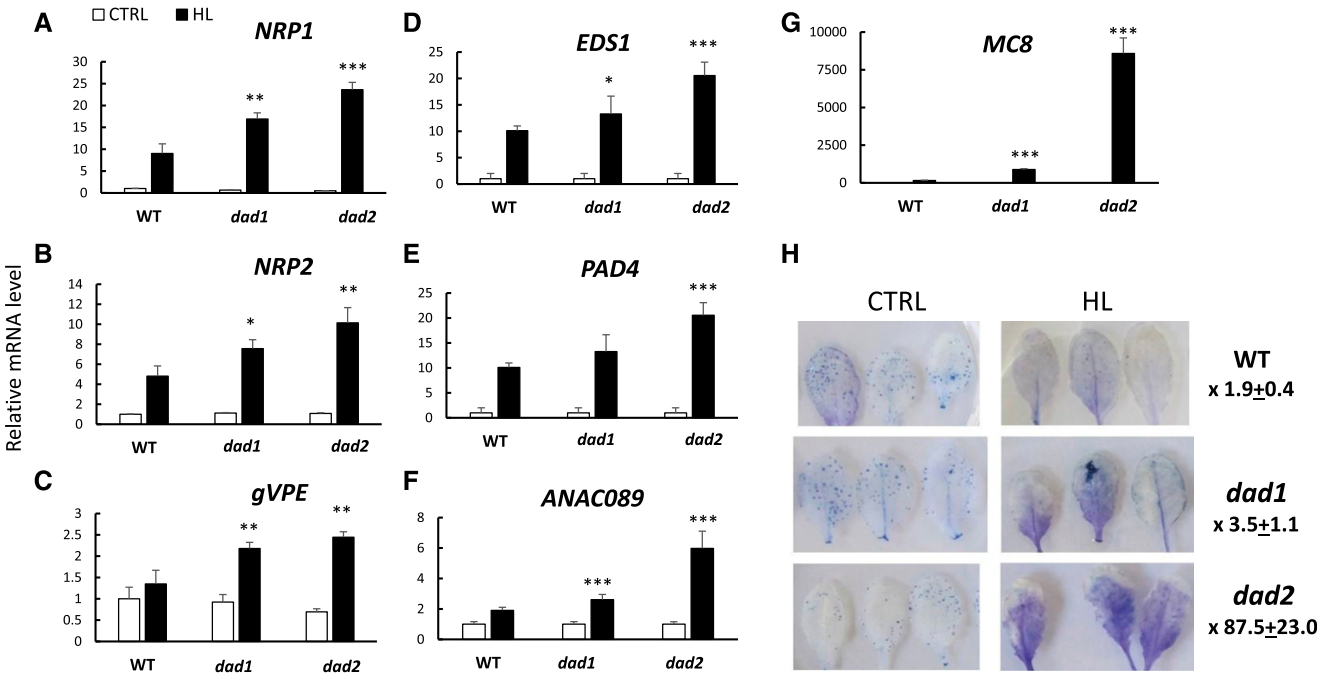

Figure 8. The *dad1* and *dad2* KO mutants exhibit an increased sensitivity to high light-induced cell death. Plants were exposed to high light (HL) stress (1,500 μmol m^{-2} s^{-1}, 7°C/18°C, day/night) for 24 h. A to G, Expression levels of PCD marker genes (*NRP1*, *NRP2*, *gVPE*, *EDS1*, *PAD4*, *ANAC089*, and *MC8*) before (CTRL) and after high light stress. *$P < 0.05$, **$P < 0.01$, and ***$P < 0.001$, compared to the wild type (WT; Student's *t* test). H, Extent of cell death as estimated by Trypan Blue staining in leaves of wild-type, *dad1*, and *dad2* plants before and after high light stress. The stained area in HL-treated leaves was scored by Image J software and was expressed as fold change over control. High light-stressed *dad* leaves with an increased blue coloration correspond to the damaged leaves shown in Fig. 7C, characterized by a high autoluminescence emission and a flaccid appearance.

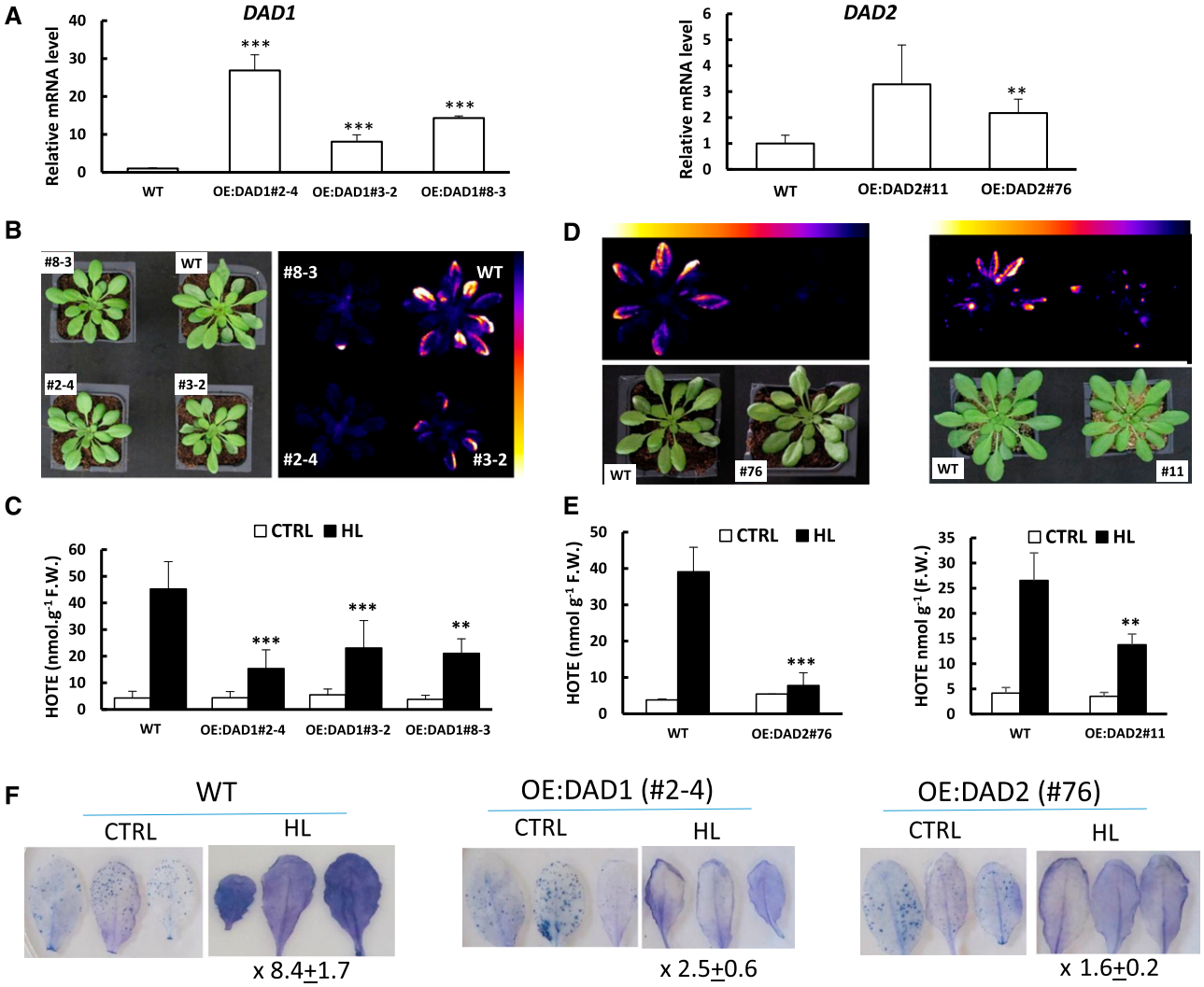

Figure 9. Overexpressing *DAD1* and *DAD2* increases tolerance to photooxidative stress. A, RT-qPCR analysis of the overexpression of *DAD1* and *DAD2* in several OE:DAD1 and OE:DAD2 lines ($n = 3$). B, Phenotype and autoluminescence imaging of wild-type (WT) Arabidopsis and three OE::DAD1 lines (2-4, 3-2, and 8-3) after 28 h of high light (HL) stress (1,500 μmol m^{-2} s^{-1} 7°C/18°C day/night). The experiment was stopped when symptoms of leaf damage and photooxidative stress were visible on wild-type leaves (28 h treatment). Please note that wild-type leaves were more stressed in this experiment than in the experiments reported in Figures 7 and 8 (28 h versus 24 h light stress in Figs. 7 and 8). The color palette indicates luminescence intensity from low (dark blue) to high values (white). C, HOTE levels before (CTRL) and after high light stress (for wild type, line 2-4, and line 3-2, $n = 10$; for line 8-3, $n = 4$) F.W., fresh weight. D, Phenotype and autoluminescence imaging of wild-type Arabidopsis and two OE:DAD2 lines (76 and 11) after 2 d of HL stress (1,500 μmol m^{-2} s^{-1} 7°C/18°C day/night). The color palette indicates luminescence intensity from low (dark blue) to high values (white). E, HOTE levels before (CTRL) and after (HL) high light stress (wild type and OE:DAD2 lines 76 and 11, $n = 4$). $^{**}P < 0.01$ and $^{***}P < 0.001$ compared to the wild type (Student's *t* test). F, Extent of cell death as estimated by Trypan Blue staining in leaves of wild-type, OE:DAD1 (line 2-4), and OE:DAD2 (line 76) plants before and after high light stress. The stained area in high light-treated leaves was scored by Image J software and was expressed as fold change over control. The high light-stressed wild-type leaves with a dark blue coloration correspond to the strongly damaged leaves shown in Fig. 9B, characterized by a high autoluminescence and a flaccid appearance.

DAD-deficient mutants and the DAD-overexpressing lines indicate that both DAD1 and DAD2 preclude cell death and mitigate photooxidative damage. The effect of *OXI1* and of the two *DAD* genes on the responses of Arabidopsis to high light stress are thus antagonistic, with DAD1 and DAD2 being negative regulators of PCD and OXI1 being a positive regulator.

We also analyzed reduced and oxidized glutathione (GSH and GSSG) levels as markers of leaf redox status (Noctor et al., 2012) in high light-stressed leaves. Supplemental Figure S4 shows that the total glutathione content (GSH+GSSG) did not differ significantly between the wild type, the *dad* mutants, and the OE:DAD transgenics. Moreover, the reduction status of

the glutathione pool was not significantly modified by *DAD1* or *DAD2* upregulation or downregulation. A similar response was previously reported in several Arabidopsis antioxidant mutants exposed to comparable light stress conditions (Müller-Moulé et al., 2003).

The question arises as to whether the anti-PCD function of the DAD proteins is specific to high light stress conditions. We tested the effects of other environmental constraints, such as heat stress and drought stress in low light, on Arabidopsis plants, and we did not find any link between DAD1 or DAD2 levels and leaf damage (Supplemental Figs. S5 and S6): wild type, *dad* KO mutants, and DAD overexpressors did not differ in terms of visual symptoms of leaf damage and lipid peroxidation after drought stress or heat stress. This suggests that DAD1 and DAD2 do not play a major regulatory role in cell death induced by those stress conditions, supporting the idea of a specific role in plant responses to radiation, both in the visible wavelength domain (this study) and in the UV spectral region (Danon et al., 2004). However, Arabidopsis root cell death induced by a mutualistic fungus is exacerbated in a DAD1-deficient mutant (Qiang et al., 2012). $^1O_2$ and $^1O_2$-induced lipid oxidation products have emerged as components of plant responses to pathogens (Vellosillo et al., 2010), providing a possible link between responses to high light and defenses against pathogens.

DAD and *OXI1* Are Regulated in an Opposite Manner and Have Antagonistic Effects on Hormones

We looked at the expression of *OXI1* in the *dad* mutants and in the *DAD* overexpressors exposed to high light stress (Fig. 10). *OXI1* expression was more induced in the *dad1* and *dad2* KO mutants than in the wild type (Fig. 10A). In contrast, *DAD1* and *DAD2* overexpression in the OE:DAD1 lines 2 to 4 and OE:DAD2 line 76 drastically downregulated the expression of *OXI1* (Fig. 10B). These results indicate that OXI1 and DAD are antagonists and suggest that the *DAD* genes negatively control the expression of *OXI1*. We also found that DAD levels modulate the jasmonate contents in parallel with the changes in OXI1 expression levels (Fig. 10C), in line with the OXI1-mediated regulation of jasmonate shown in Figure 3A.

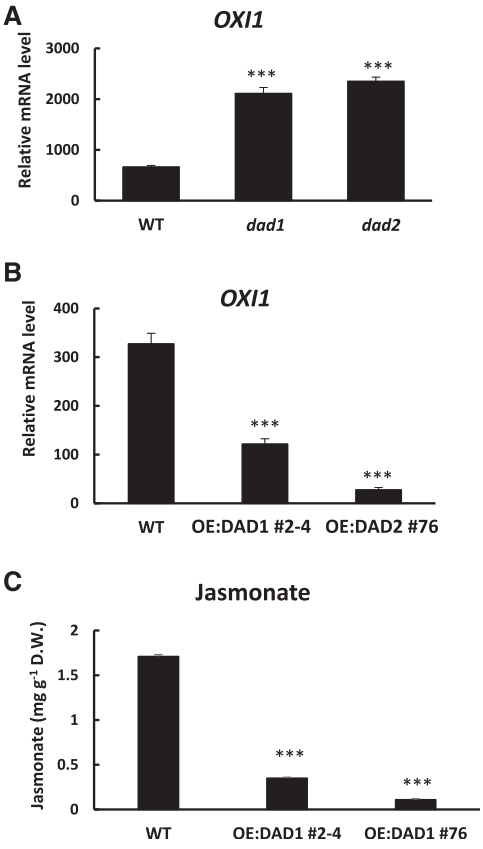

Figure 10. *OXI1* expression levels in the *dad1* and *dad2* KO mutants and in OE:DAD1 and OE:DAD2 lines. A, RT-qPCR analysis of *OXI1* expression levels in wild-type (WT) Arabidopsis and in the *dad1* and *dad2* mutants after high light (HL) stress. Data are normalized on the levels before stress ($n = 3$). B, RT-qPCR analysis of *OXI1* expression levels in OE:DAD1 and OE:DAD2 lines (2-4 and 76, respectively) after HL stress conditions. Data are normalized to the control wild-type levels ($n = 3$). C, Jasmonate levels in wild-type Arabidopsis and in the OE:DAD1 line 2-4 and OE:DAD2 line 76 after high light stress ($n = 3$). D.W., dry weight. ***$P < 0.001$, compared to the wild type (Student's *t* test).

Gene Regulation by Jasmonate and Salicylate

We examined the effects of jasmonate or salicylic acid treatments on the expression of the *DAD* and *OXI1* genes. Spraying wild-type plants with 1 mM jasmonate induced the expression of *OXI1*, whereas both *DAD1* and *DAD2* were down-regulated (Fig. 11A). In contrast, 1 mM salicylic acid induced *DAD1* and *DAD2* expression while *OXI1* expression was not affected (Fig. 11B). Thus, *DAD* and *OXI1* were differentially responsive to hormones and behaved in an almost opposite manner. Moreover, there was a feedback effect of jasmonate on *OXI1*, since this gene at the same time controls jasmonate biosynthesis (Fig. 3) and is up-regulated by jasmonate (Fig. 11A). The expression of *DAD1* is down-regulated with the onset of PCD (Moharikar et al., 2007), and this could explain the repression of *DAD1* by 1 mM jasmonate (Fig. 11A), a concentration that was found to induce leaf damage and cell death in wild-type Arabidopsis plants (Fig. 12, A–D). In Supplemental Figure S7, we compare the expression of *DAD1* and *DAD2* in OE:OXI1, OE:OXI1 x *sid2*, and OE:OXI1 *dde2*. The *sid2* mutation, not the *dde2* mutation, inhibited the expression of both *DAD1* and *DAD2*, confirming the control of those genes by salicylate.

In this study, jasmonate and salicylic acid increased and decreased concomitantly when *OXI1* expression was high and low, respectively (Figs. 3 and 10). To evaluate the hierarchy of those hormonal changes in

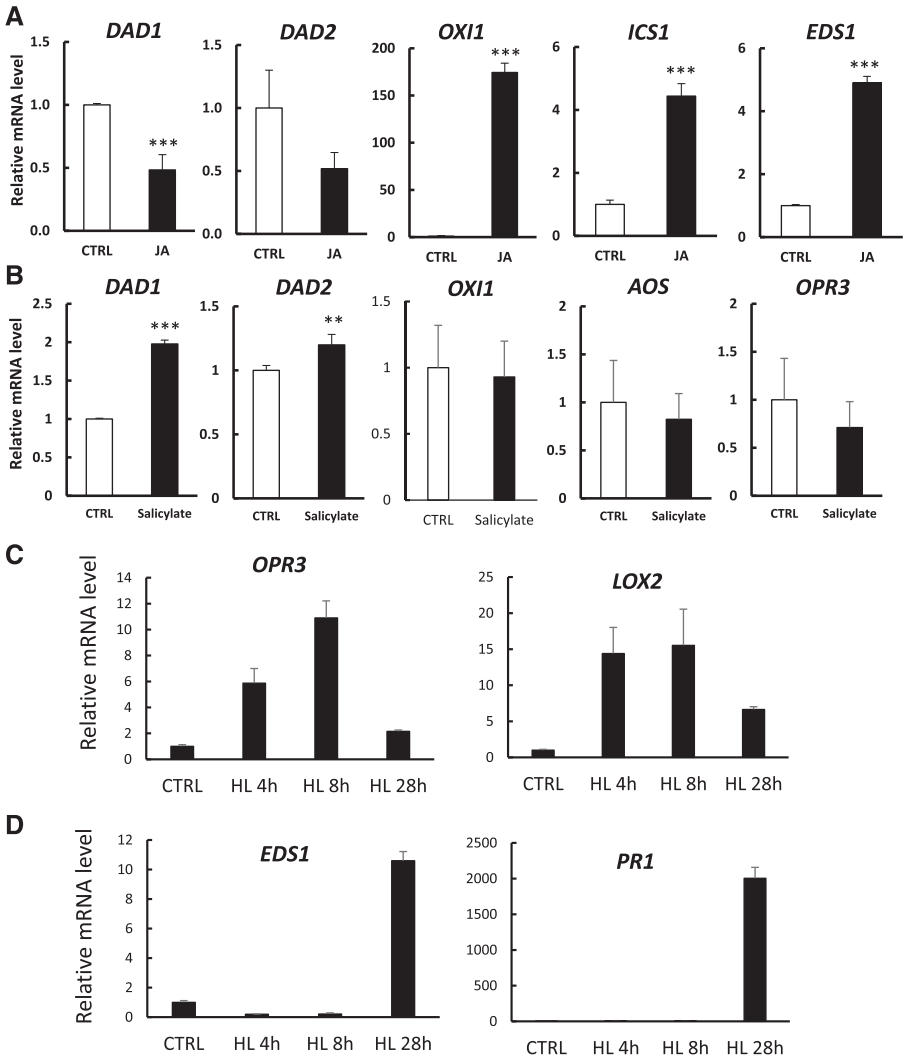

Figure 11. Hormone regulation by OXI1 and DAD. A, RT-qPCR analysis of *OXI1*, *DAD1*, *DAD2*, and genes of the salicylate signaling pathway (*EDS1* and *ICS1*) after treatment of wild-type plants with 1 mM methyl jasmonate ($n = 3$). B, RT-qPCR analysis of *OXI1*, *DAD1*, *DAD2*, and genes of the jasmonate biosynthesis pathway (*AOS* and *OPR3*) after treatment of wild-type Arabidopsis with 1 mM salicylate ($n = 3$). C and D, Time courses of expression of jasmonate biosynthesis genes (C; *LOX2* and *OPR3*) and salicylate-related genes (D; *ICS1* and *PR1*) upon transfer of Arabidopsis plants from low light (CTRL) to high light (HL). $^{**}P < 0.01$ and $^{***}P < 0.001$, compared to control condition (Student's *t* test).

our conditions, we examined the effect of one hormone on the expression of the biosynthesis pathway of the other hormone. Figure 11A shows that jasmonate induced the expression of the salicylic acid biosynthesis genes, *EDS1* and *ISOCHORISMATE SYNTHASE1* (*ICS1*). In contrast, salicylic acid had no significant effect on genes involved in the jasmonate biosynthesis pathway, *AOS* and *OPR3* (Fig. 11B). These results suggest that, in high light stress, the accumulation of jasmonate leads to an increase in salicylic acid by regulating its biosynthesis. We also examined the time course of expression of genes related to jasmonate or salicylate biosynthesis/signaling after transfer of Arabidopsis plants from low light to high light (Fig. 11, C and D). Interestingly, the jasmonate biosynthesis genes, *LOX2* and *OPR3*, were induced after 4 h illumination. In contrast, induction of the salicylate-related genes, *EDS1* and *PR1*, was noticeably slower, occurring after 26 h in high light. Moreover high light-induced expression levels of PR1 were considerably higher than those of the jasmonate biosynthesis genes. This delay of several hours in the induction of the two classes of genes is in line with an upstream position of jasmonate relative to salicylate in the signaling pathway.

Jasmonate-induced cell death was dependent on salicylic acid. When plants were treated with 1 mM jasmonate, leaf damage occurred within 24 h. When the same treatment was applied to the salicylic acid mutant *sid2*, cell death was strongly attenuated: considerably fewer leaves showed visual symptoms of damage (Fig. 12, A–C), and cell membrane disruption and trypan blue staining were markedly attenuated (Fig. 12, D and E). Jasmonate-induced damage appeared as flaccid and darkened leaf areas, which were quantified using Image J software (Fig. 12, B and C). These results support the idea that jasmonate controls $^1O_2$-induced PCD through salicylic acid. Furthermore, we found that the *sid2* mutant was more resistant to high light stress than the wild type (Fig. 12, F and G). When exposed to photooxidative stress conditions, *sid2* plants exhibited less lipid peroxidation compared to wild-type plants, indicating salicylic acid has an essential role in the induction of photodamage. The same phenomenon was observed in the photosensitive *ch1* genetic background

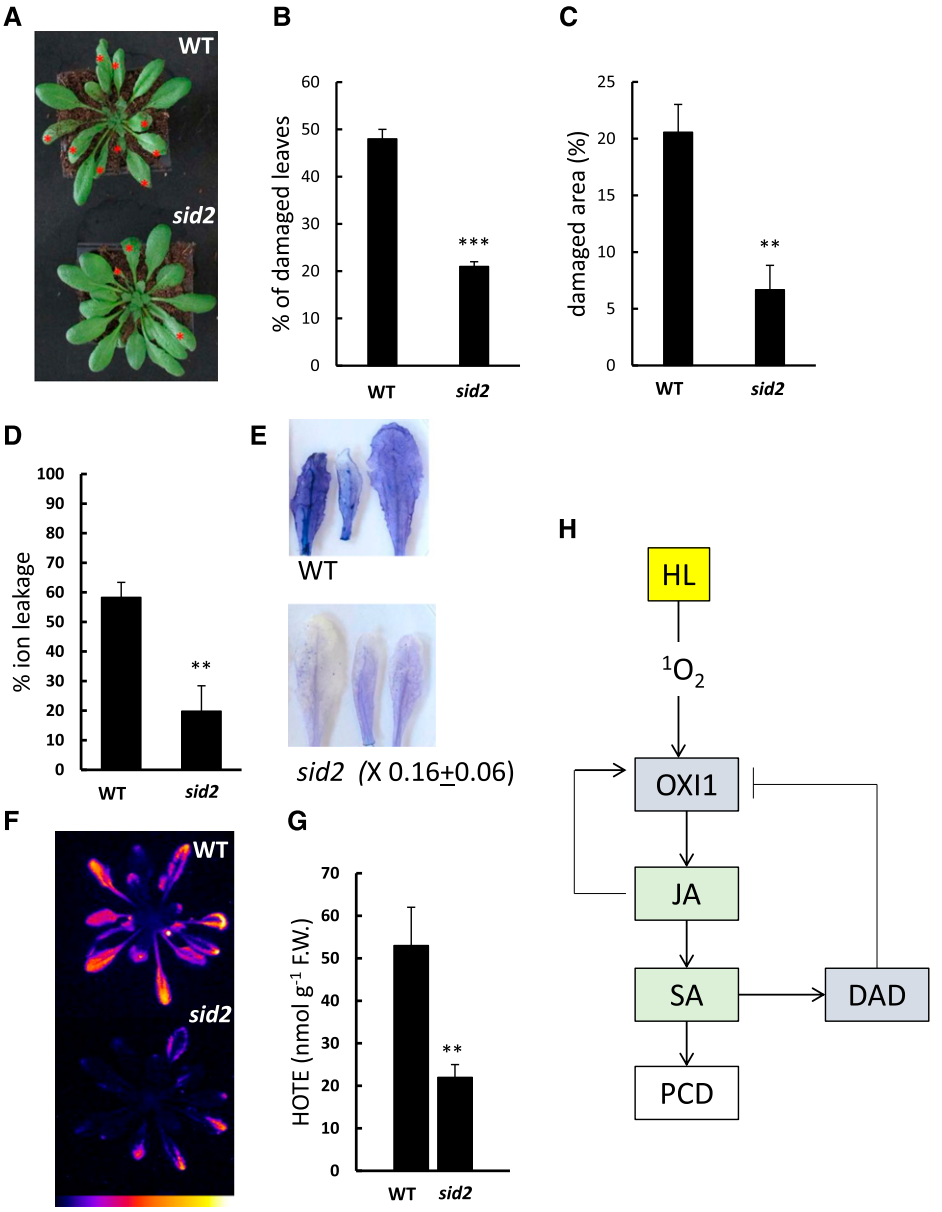

Figure 12. Effects of the *sid2* mutation on high light- and jasmonate-induced cell death. A to D, Effects of 1 mM methyl jasmonate (24 h) on wild-type (WT) and *sid2* Arabidopsis plants. Red stars in A indicate leaves with visible damage. Leaf damage was analyzed by Image J software to determine the number of damaged leaves (relative to the total number of leaves; B) and the damaged area in each leaf (relative to the total leaf area; C). Electrolyte leakage from leaves in distilled water is shown in D ($n = 3$). E, Extent of cell death as estimated by Trypan Blue staining in wild-type and *sid2* leaves after the 24-h jasmonate treatment. The stained area in *sid2* leaves was scored by Image J software and was expressed as fold change over the wild type. The leaves used for the staining correspond to the leaves marked with the red stars (A). F and G, Effects of high light stress (1,500 μmol photons m^{-2} s^{-1} at 7°C for 2 d) on wild-type and *sid2* Arabidopsis plants. Lipid peroxidation was measured by autoluminescence imaging (F; the color palette indicates luminescence intensity from low [dark blue] to high values [white]) and quantification of HOTE levels (G) after high light stress ($n = 3$). F.W., fresh weight. H, Scheme of the proposed regulation of PCD by OXI1 and DAD via jasmonate (JA) and salicylate (SA) under high light (HL) conditions. B and C, $^{**}P < 0.01$ and $^{***}P < 0.001$, compared to the wild type (Student's *t* test).

in which $^1O_2$ release by the PSII centers is strongly increased (Ramel et al., 2013a). The *sid2* mutation noticeably reduced the $^1O_2$-induced oxidative photodamage in *ch1* leaves (Supplemental Fig. S8).

DISCUSSION

Role of Jasmonate and Salicylate in the Response of Arabidopsis to Photooxidative Stress

This work has confirmed the role of jasmonate in high light-induced cell death (Ramel et al., 2013a, 2013b) and the modulating effect of the OXI1 protein on this pro-death mechanism (Shumbe et al., 2016). In fact, overexpression of *OXI1* concomitantly induced jasmonate accumulation and PCD. When jasmonate biosynthesis was inhibited by the *dde2* mutation in the *OXI1* overexpressors, the enhancement of senescence and PCD was cancelled, demonstrating a causal link between jasmonate biosynthesis and those phenomena. OXI1 is an AGC kinase that can phosphorylate several target proteins (Howden et al., 2011). One of the identified targets is a phospholipase D-γ, an enzyme that has previously been reported to participate in wound-induced jasmonate biosynthesis, possibly through a regulatory effect on lipoxygenase LOX2 expression (Wang et al., 2000). It is thus a possible player in the OXI1-dependent induction of jasmonate accumulation. Interestingly, the phosphoproteome of the *oxi1* mutant has also revealed a decrease in the phosphorylation of ETHYLENE INSENSITIVE2 compared to the wild type (Howden et al., 2011). ETHYLENE INSENSITIVE2 is necessary for ethylene-induced gene regulation and has

been recognized as a molecular link between several hormone response pathways, including the jasmonate signaling pathway (Alonso et al., 1999). OXI1 is also known to be essential for the full activation of MPK3 and MPK6 in response to H_2O_2 and to pathogens (Rentel et al., 2004), and MPK6 plays a role in regulating jasmonate-induced leaf senescence (Zhou et al., 2009). However, *MPK3* and *MPK6* are not induced by $^1O_2$ (Shumbe et al., 2016) and are not upregulated in the OE:OXI1 plants (Supplemental Fig. S3).

Besides phosphorylation-based regulation of the activity of specific proteins linked to jasmonate synthesis/signaling, OXI1 could also act on jasmonate biosynthesis. Shumbe et al. (2016) found that several jasmonate biosynthesis genes, such as *AOS* and *OPR3*, are downregulated in the *oxi1* KO mutant compared to the wild type. Figure 3, E and F, shows that the jasmonate biosynthesis genes *OPR3* and *LOX2* were markedly upregulated in OE:OXI1 plants, confirming the link between OXI1 expression and jasmonate levels.

This work also points out the role of another phytohormone, salicylate, in OXI1-mediated PCD in high light, downstream of jasmonate. *OXI1* expression levels changed in parallel with salicylate levels, and blocking salicylate biosynthesis inhibited OXI1-mediated PCD. In agreement with those results, the control of the salicylate biosynthesis pathway by OXI1 in Arabidopsis was previously reported in a study of the induction of defense signaling by melatonin (Lee and Back, 2017). Moreover, inhibition of jasmonate synthesis by the *dde2* mutation in the OE:OXI1 plants suppressed both PCD and salicylate synthesis. Also, the salicylate-deficient mutant *sid2* was much more resistant to high light stress compared to the wild type, confirming the essential role of salicylate in the development of cellular photooxidative damage. The role of salicylic acid in the induction of PCD is well established in the context of pathogen defense responses (Gaffney et al., 1993; Lawton et al., 1995; Alvarez, 2000; Vlot et al., 2009,). The coaction of jasmonate and salicylate in the light-induced death response is in agreement with a previous study of the $^1O_2$-producing Arabidopsis *flu* mutant, which showed a reduced extent of $^1O_2$-induced cell death by expressing transgenic *NahG* or by crossing *flu* with the *dde2* mutant (Danon et al., 2005). Our results are also consistent with previous works on the Arabidopsis *catalase2* mutant showing the simultaneous activation of the salicylate and jasmonate pathways by intracellular oxidative stress (Noctor et al., 2015). Binding of salicylic acid to its receptors NPR3 and NPR4 in a concentration-dependent manner modulates their interaction with NPR1, hence determining the NPR1-dependent defense response (Moreau et al., 2012). However, contrary to the *sid2* mutant, the *npr1* KO mutant was not more tolerant to high light stress at low temperature than the wild type (Supplemental Fig. S9). This indicates that salicylate-mediated PCD under high light does not occur primarily through the NPR1-mediated pathway.

Exposure of Arabidopsis to high light stress conditions leading to cell death was associated with the concomitant accumulation of jasmonate and salicylate. The jasmonate and salicylate signaling pathways interact with each other in the induced resistance to pathogens, sometimes resulting in antagonistic effects (Caarls et al., 2015). This hormonal antagonism does not seem to occur under high light conditions, since cell death was prevented when biosynthesis of each of the two hormones was individually inhibited, indicating that both hormones are required for cell death under those conditions. Interestingly, treatment of plants with jasmonate upregulated genes of the salicylate pathway, whereas, in contrast, treatment with salicylate had no such effect on jasmonate biosynthesis genes. Therefore, jasmonate appears to act upstream of salicylate in the response to high light stress. This differs from the inducible immune response in which salicylate has been proposed to take control over jasmonic acid signaling (Caarls et al., 2015).

DAD1 and DAD2 Are Negative Regulators of High Light-Induced Cell Death

An important result of this study is the discovery of a negative regulator of high light-induced PCD. DAD-deficient and DAD-overexpressing Arabidopsis lines behaved in an opposite manner to the *oxi1* KO mutant and OE:OXI1 plants, in terms of both phototolerance and jasmonate levels. The phototolerance phenotype of the OE:DAD1 and OE:DAD2 plants shows that both DAD proteins are involved in the mitigation of high light-induced cell damage. In this context, we can mention a previous study of protoplasts exposed to UV radiation in which expression of the Arabidopsis DAD1 or DAD2 proteins suppressed cell death (Danon et al., 2004). In the microalga *Chlamydomonas reinhardtii*, a correlation was found between UV-induced cell death and downregulation of *DAD1* (Moharikar et al., 2007). Importantly, we also found an antagonistic effect between expression of *DAD1* and expression of *OXI1*. Increasing the expression of *DAD1* or *DAD2* brought about a marked repression of *OXI1*. Conversely, *OXI1* was upregulated in the *dad1* and *dad2* KO mutants. In contrast, changing the *OXI1* expression levels had limited effects on *DAD1* and *DAD2* gene expression. These observations suggest a control of *OXI1* expression by *DAD1* and *DAD2*, and therefore the anti-PCD action of DAD could occur through modulation of the pro-PCD activity of OXI1.

The amino acid sequence of DAD1 is highly conserved through the plant and animal kingdoms. In animals, DAD1 is part of the N-glycosylation complex in the ER (Makishima et al., 1997). N-glycosylation is a major class of posttranslational protein modifications in eukaryotic cells ensuring the proper folding and maturation of nascent proteins in the ER (Strasser, 2016). There is a link between N-glycosylation and apoptosis, as illustrated by the use of the N-glycosylation inhibitor

tunicamycin as an assay of apoptosis (Dricu et al., 1997; Yoshimi et al., 2000). The function of Arabidopsis DAD1 seems to be similar to the function of DAD1 in animals since it can complement a hamster (*Mesocricetus auratus*) apoptosis suppressor mutant (Gallois et al., 1997). As a component of the glycosylation complex, DAD1 may target specific proteins that directly maintain cell survival. Another possibility is that accumulation of unfolded or misfolded proteins consecutive of hypoglycosylation at the ER in the *dad* KO mutants triggers stress signaling and initiates PCD (Haynes et al., 2004). It is well known that high light stress generates ROS in the chloroplasts, leading to cellular oxidative stress (Asada, 2006; Li et al., 2009), and proteins are one of the prime targets for oxidative damage, for example through oxidation of Cys residues (Gracanin et al., 2009; Akter et al., 2015). Oxidation of thiol groups in proteins may lead to protein malfolding (Rakhit et al., 2002; Goldberg, 2003). Consequently, under photooxidative stress conditions, excessive accumulation of misfolded proteins in the ER, a phenomenon known as ER stress, can trigger PCD (Sano and Reed, 2013). Accumulation of unfolded proteins in the *dad* KO mutants would accelerate this phenomenon, whereas overexpression of *DAD1* and *DAD2* is expected to boost the protein folding mechanism, thus preventing ER stress and PCD. In Supplemental Figure S10, we compare the expression of several genes involved in the ER stress response: *BASIC REGION/LEUCINE ZIPPER MOTIF 60* (*bZIP60*), bZIP*28*, and *BINDING PROTEIN 3*, in wild-type, OE:DAD1, and OE:DAD2 plants exposed to high light stress. High DAD levels lowered transcript levels of those genes, suggesting a reduced ER stress. Involvement of the ER-resident DAD proteins in the response to high light stress is consistent with recent findings emphasizing the role of chloroplast-to-ER signaling in stress adaptation of plants (Walley et al., 2015; de Souza et al., 2017).

It is difficult to say how the reported glycosylation function of DAD1 is linked with DAD-mediated regulation of *OXI1* expression in Arabidopsis. However, glycosylation can target a large variety of proteins, including transcription factors, and there are reports of N-glycosylation of transcription factors involved in cell death regulation in mammals: for instance, in the human pancreas, glycosylation of the Sp1 transcription factor causes cancer cell death (Banerjee et al., 2013). However, contrary to mutations in other components of the plant glycosylation complex, mutations of the individual DAD genes produce very weak growth/underglycosylation phenotypes (Jeong et al., 2018), which could suggest redundant functions of DAD1 and DAD2 in this complex. However, this is not consistent with the observation that the single mutants *dad1* and *dad2* are both sensitive to photooxidative stress, indicating that each individual DAD gene plays a specific role in PCD. Consequently, one cannot exclude that the DAD proteins have a function other than glycosylation or are multifunctional proteins in plants with a specific function in PCD gene regulation different from N-glycosylation. Accordingly, the mammalian DAD1 interacts with a Bcl2 family protein, MCL1 Apoptosis Regulator, which is known to prevent cell death (Makishima et al., 2000).

In summary, we have identified two cell death regulators, OXI1 and DAD, which have opposite effects in the response of Arabidopsis to high light stress. The development of high light-induced cell death must therefore result from a tight control of the relative activities of these regulating proteins. In Figure 12H, the main results of this study are integrated in a model of OXI1-dependent PCD in plants exposed to photooxidative stress conditions. Induction of *OXI1* expression leads to PCD through sequential enhancement of jasmonate and salicylate syntheses. Since *OXI1* expression is stimulated by jasmonate, we can propose a positive feedback loop amplifying the OXI1-dependent signaling pathway and the associated hormone accumulations. The anti-PCD regulators DAD1 and DAD2 provide a negative feedback loop to avoid erratic and undesirable overactivity of the OXI1-dependent pathway, as observed in the OE:OXI1 plants that exhibit a premature senescence phenotype. Finally, a complex interplay between the antagonistic actions of cell death regulators, in which modulation of jasmonate and salicylate levels plays an important role, determines orientation of the response of plants to high light toward cell death or acclimation.

MATERIALS AND METHODS

Plant Material, Growth Conditions, and Stress Treatments

Arabidopsis (*Arabidopsis thaliana*) plants were grown in a phytotron under controlled temperature (20°C/18°C, day/night), PFD (150 μmol photons m^{-2} s^{-1}, 8 h photoperiod) and relative air humidity (65%). Unless specified otherwise, plants aged 5 weeks were used for the experiments. The experiments were performed on wild type Arabidopsis (ecotype Columbia-0) and transfer DNA insertion mutants *dad1* (Sail_828_C02), *dad2* (Salk_015587) and *oxi1* (Shumbe et al., 2016). Genotyping was performed using full-length coding sequence primers designed for cloning on complementary DNA (cDNA; Supplemental Table S1). *35S:DAD1* and *35S:DAD2* overexpression constructs were made by inserting the coding region of *DAD1* and *DAD2* amplified by PCR using DAD1-attB-LP; DAD1-attB-RP and DAD2-attB-LP; DAD2-attB-RP into pB2GW7 via the GATEWAY cloning system (Dubin et al., 2008). For OE:OXI1 lines (35 and 8054), a 2.2 Kb region upstream of the *OXI1* gene, the genomic sequence of *OXI1* with the 5′ untranslated transcribed region, and the 3′ untranslated transcribed region were amplified by PCR and cloned in the pCambia 3300 (*Eco*RI-*Nhe*I/*Xba*I) vector. The Human influenza hemagglutinin tag was cloned at the *Sal*I site found at the ATG site of *OXI1*. Transgenic plants were obtained by *Agrobacterium tumefaciens*-mediated floral dip (Clough and Bent, 1998) in Col-0 background and identified by RT-qPCR.

OE:OXI1 lines 35 and 8054 were crossed with the salicylic acid-deficient mutant *sid2-2* (Wildermuth et al., 2001) or with the jasmonate-depleted mutant *dde2* (von Malek et al., 2002). The selection of homozygous double mutant plants was achieved by selecting plants that showed 100% resistance to the herbicide BASTA (Bayer), which were subsequently screened for the mutation by RT-PCR.

Photooxidative stress was induced in plants by exposing them to 1,500 μmol photons m^{-2} s^{-1} PFD, 7°C/18°C day/night temperature, and 380 ppm CO_2 in a growth chamber for several durations specified in the figure legends, using the Phytotec platform at the Commissariat à l'Energie Atomique et aux Energies Alternatives of Cadarache. Heat stress was imposed by transferring plants to a growth chamber at 48°C (air temperature) and low PFD

(100 μmol photons m^{-2} s^{-1}) for 1.5 h, as described elsewhere (Boca et al., 2014). Drought stress was induced in low light (150 μmol photons m^{-2} s^{-1}) by withdrawing watering for 12 d.

Lipid Peroxidation Quantification and Imaging

Lipids were extracted from ~0.5 g of leaves frozen in liquid nitrogen. The leaves were ground in an equivolume methanol/chloroform solution containing 5 mM triphenyl phosphine, 1 mM 2,6-tert-butyl-p-cresol (5 mL g^{-1} fresh weight), and citric acid (2.5 mL g^{-1} fresh weight), using an Ultra-Turrax blender (IKA-Werke). Internal standard 15-Hydroxy-eicosadienoic acid was added to a final concentration of 100 nmol g^{-1} fresh weight and mixed properly. After centrifugation at 700 rpm and 4°C for 5 min, the lower organic phase was carefully collected with the help of a glass syringe into a 15-mL glass tube. The syringe was rinsed with 2.5 mL of chloroform and transferred back into the tube. The process was repeated, and the lower layer was again collected and pooled to the first collection. The solvent was evaporated under N_2 gas at 40°C. The residues were recovered in 1.25 mL of absolute ethanol and 1.25 mL of 3.5 N NaOH and hydrolyzed at 80°C for 30 min. The ethanol was evaporated under N_2 gas at 40°C for 10 min. After cooling to room temperature, the pH was adjusted to 4 to 5 with 2.1 mL of citric acid. Hydroxy fatty acids were extracted with hexane/ether (50/50, v/v). The organic phase was analyzed by straight-phase HPLC-UV, as previously described (Montillet et al., 2004). HOTE isomers (9-, 12-, 13-, and 16-HOTE derived from the oxidation of the main fatty acid in Arabidopsis leaves, linolenic acid) were quantified based on the 15-Hydroxy-eicosadienoic acidinternal standard. Lipid peroxidation was also visualized in whole plants by autoluminescence imaging. Stressed plants were dark adapted for 2 h, and the luminescence emitted from the spontaneous decomposition of lipid peroxides was captured by a highly sensitive liquid N_2-cooled charge coupled device camera, as previously described (Birtic et al., 2011). The images were analyzed using Image J software (National Institutes of Health).

Trypan Blue Staining

Detached leaves were stained with Trypan Blue (1 mg mL^{-1}) to evaluate the extent of leaf cell death according to Fernandez-Bautista et al. (2016). The Trypan Blue solution was prepared by dissolving 40 mg Trypan Blue in 10 mL lactic acid (85%, w/w), 10 mL phenol (buffer equilibrated, pH 7.5–8.0), 10 mL glycerol, and 10 mL distilled water. Leaves were incubated in the Trypan Blue solution for 40 min, then immediately rinsed with ethanol and washed overnight in ethanol.

RNA Isolation and RT-qPCR

Total RNA was isolated from 200 mg of leaves by adding 500 μL TRI-reagent and 200 μL chloroform (SigmaAldrich). Adding ethanol absolute (v/v) to the supernatant allowed for transferal to a violet column of the Nucleospin RNA plant kit (Macherey-Nagel). The concentration was measured on a NanoDrop2000 (Thermo Fisher Scientific). First-strand cDNA was synthesized from 3 μg of total RNA using the PrimeScript reverse transcriptase kit (Takara). RT-qPCR was performed on a real-time PCR instrument (Roche LightCycler 480 system). Six microliters of a reaction mixture comprising SYBR Green I Master (Roche) and 10 μM forward and reverse primers (5:1) were added to 4 μL of 10-fold diluted cDNA sample in a 384-well plate. The PCR program used was as follows: 95°C for 10 min, then 45 cycles of 95°C for 15 s, 60°C for 15 s, and 72°C for 15 s. Primers for genes studied (Supplemental Table S1) were designed using the Universal Probe Library (Roche; https://lifescience.roche.com/en_fr/brands/universal-probe-library.html).

Hormone Quantification

Endogenous levels of jasmonates (jasmonic acid [JA]; Jasmonoyl-L-Ile [JA-Ile]; cis-12-oxo-phytodienoic acid [cis-OPDA]) and salicylic acid (SA) were determined in 20 mg of fresh plant material according to the method described by Floková et al. (2014). The phytohormones were extracted using an aqueous solution of methanol (10% [v/v] MeOH/H_2O). A cocktail of stable isotope-labeled standards was added as follows: 10 pmol of [$^2H_6$]JA and [$^2H_2$]JA-Ile and 20 pmol of [$^2H_4$]SA and [$^2H_5$]OPDA (all from Olchemim Ltd.) per sample to validate the liquid chromatography-mass spectrometry (LC-MS) method. The extracts were purified using Oasis hydrophilic-lipophilic balanced columns (30 mg/1 mL; Waters), and targeted analytes were eluted using 80% MeOH (v/v). Eluent containing neutral and acidic compounds was gently evaporated to dryness under a stream of nitrogen. Separation was performed on an Acquity Ultra High Performance LC (UPLC) System (Waters) equipped with an Acquity UPLC BEH C18 column (100 × 2.1 mm, 1.7 μm; Waters), and the effluent was introduced into the electrospray ion source of a triple quadrupole mass spectrometer Xevo TQ-S MS (Waters).

Some analyses of jasmonate and salicylate levels were also performed on freeze-dried leaf powder by UPLC-tandem MS by the "Plateforme de Chimie du Végétal" at the Institut Jean-Pierre Bourgin. For each sample, 3 mg of dry powder was extracted with 0.8 mL of acetone:water:acetic acid (80:19:1 [v/v/v]). Salicylic acid and jasmonic acid stable labeled isotopes used as internal standards were prepared as described in Le Roux et al. (2014). Two ng of each standard was added to the sample. The extract was vigorously shaken for 1 min, sonicated for 1 min at 25 Hz, shaken for 10 min at 10°C in a Thermomixer (Eppendorf), and then centrifuged (8,000 × g, 10°C, 10 min). The supernatants were collected, and the pellets were re-extracted twice with 0.4 mL of the same extraction solution, then vigorously shaken (1 min) and sonicated (1 min; 25 Hz). After the centrifugations, the three supernatants were pooled and dried (Final Volume 1.6 mL).

Each dry extract was dissolved in 100 μL of acetonitrile:water (50:50 v/v), filtered, and analyzed using a Acquity ultra performance liquid chromatograph (Waters) coupled to a Xevo TQ-S Triple quadrupole mass spectrometer (UPLC-electrospray ionization-tandem MS; Waters). The compounds were separated on a reverse-phase column (Uptisphere C18 UP3HDO, 100 × 2.1 mm and 3 μm particle size; Interchim) using a flow rate of 0.4 mL min^{-1} and a binary gradient: (A) acetic acid 0.1% (v/v) in water and (B) acetonitrile with 0.1% (v/v) acetic acid. The column temperature was 40°C. For abscisic acid, salicylic acid, jasmonic acid, and indole-3-acetic acid we used the following binary gradient (time, % of phase A: 0 min, 98%; 3 min, 70%; 7.5 min, 50%; 8.5 min, 5%; 9.6 min, 0%; 13.2 min, 98%; and 15.7 min, 98%). MS was conducted in electrospray and multiple reaction monitoring scanning mode, in positive ion mode for the indole-3-acetic acid, and in negative ion mode for the other hormones. Relevant instrumental parameters were set as follows: capillary 1.5 kV (negative mode), and source block and desolvation gas temperatures 130°C and 500°C, respectively. Nitrogen was used to assist the cone and desolvation (150 L h^{-1} and 800 L h^{-1}, respectively), and argon was used as the collision gas at a flow of 0.18 mL min^{-1}.

Ion Leakage Measurements

Six leaves per condition were cut from plants, weighed (fresh weight), and placed in 25 mL of bidistilled water. Conductivity of the solution was measured with a DIST-5 conductometer (Hanna Instruments) after 2 h of mild agitation and after boiling the samples. The values were normalized on the fresh weight, and the values after boiling are reported as the maximal value.

Glutathione Determination

Reduced glutathione (GSH) and oxidized glutathione (GSSG) were measured by a colorimetric assay using 5-5′-dithiobis (2-nitrobenzoic acid) and the recycling method based on glutathione reductase and NADPH. Three leaf discs of 1 cm diameter were ground in 300 μL of 5% (w/v) sulfosalicylic acid in 0.1 M Na-phosphate buffer, pH 7.4. After centrifugation, the supernatant was used for glutathione analysis using the protocol detailed in Salbitani et al. (2017).

Accession Numbers

DAD1 (AT1G32210), *DAD2* (AT2G35520), *OXI1* (AT3G25250), *SID2* (AT1G74710), *DDE2* (AT5G42650)

Supplemental Data

The following supplemental materials are available.

Supplemental Figure S1. The early senescence phenotype of the OE:OXI1 lines (35 and 8054) was amplified by increasing the growth PFD (from 90 to 130 μmol photons m^{-2} s^{-1}).

Supplemental Figure S2. Phenotypes and gene expression of OE:OXI1 lines with mutations in salicylate and jasmonate biosynthesis genes.

Supplemental Figure S3. Expression levels of *MAPK3* and *MAPK6* in OXI1:OE (line 35) compared to the wild type.

Supplemental Figure S4. Glutathione concentration and reduced fractions in wild-type Arabidopsis, *dad1* and *dad2* KO mutants, and *DAD1*- and *DAD2*-overexpressing lines.

Supplemental Figure S5. Effect of heat stress (48°C for 1.5 h) in low light (100 μmol photons m^{-2} s^{-1}) on wild-type Arabidopsis, *dad1* and *dad2* KO mutants, and *DAD1*- and *DAD2*-overexpressing lines.

Supplemental Figure S6. Effect of drought stress in low light (100 μmol photons m^{-2} s^{-1}) on wild-type Arabidopsis, *dad1* and *dad2* KO mutants, and *DAD1*- and *DAD2*-overexpressing lines.

Supplemental Figure S7. Expression levels of the *DAD1* and *DAD2* genes in OE:OXI1 (line 35), OE:OXI1 × *sid2*, and OE:OXI1 × *dde2* leaves.

Supplemental Figure S8. Effect of high light stress (1,000 μmol photons m^{-2} s^{-1} at 10°C for 24 h) on the $^1O_2$-overproducing mutant *ch1* and in the double mutant *ch1*sid2*.

Supplemental Figure S9. Effects of high light stress on the *npr1* mutant compared to the wild type.

Supplemental Figure S10. Effect of high light stress (1,500 μmol photons m^{-2} s^{-1}, 7°C) on the expression of genes (*bZIP60, bZIP28*, and BINDING PROTEIN *3*) of the endoplasmic reticulum stress response in the wild type and in *DAD1*- or *DAD2*-overexpressing lines.

Supplemental Table S1. Primer sequences used in RT-qPCR transcript profiling.

ACKNOWLEDGMENTS

We thank Dr. Patrick Gallois for useful discussions, the Phytotec platform (CEA Cadarache) for growing plants under normal and stress conditions, and Hana Omámiková and Sylvie Citerne for their help with phytohormone analyses. *Sid2-2* and *npr1* seeds were a kind gift from Dr. Gerit Behtke. The *dad1* and *dad2* mutants were obtained from the Arabidopsis Biological Resource Center.

Received March 25, 2019; accepted May 7, 2019; published May 13, 2019.

LITERATURE CITED

Akter S, Huang J, Waszczak C, Jacques S, Gevaert K, Van Breusegem F, Messens J (2015) Cysteines under ROS attack in plants: A proteomics view. J Exp Bot **66:** 2935–2944

Alonso JM, Hirayama T, Roman G, Nourizadeh S, Ecker JR (1999) EIN2, a bifunctional transducer of ethylene and stress responses in Arabidopsis. Science **284:** 2148–2152

Alvarez ME (2000) Salicylic acid in the machinery of hypersensitive cell death and disease resistance. Plant Mol Biol **44:** 429–442

Alves MS, Reis PA, Dadalto SP, Faria JA, Fontes EP, Fietto LG (2011) A novel transcription factor, ERD15 (Early Responsive to Dehydration 15), connects endoplasmic reticulum stress with an osmotic stress-induced cell death signal. J Biol Chem **286:** 20020–20030

Anthony RG, Henriques R, Helfer A, Mészáros T, Rios G, Testerink C, Munnik T, Deák M, Koncz C, Bögre L (2004) A protein kinase target of a PDK1 signalling pathway is involved in root hair growth in Arabidopsis. EMBO J **23:** 572–581

Apel K, Hirt H (2004) Reactive oxygen species: Metabolism, oxidative stress, and signal transduction. Annu Rev Plant Biol **55:** 373–399

Asada K (2006) Production and scavenging of reactive oxygen species in chloroplasts and their functions. Plant Physiol **141:** 391–396

Banerjee S, Sangwan V, McGinn O, Chugh R, Dudeja V, Vickers SM, Saluja AK (2013) Triptolide-induced cell death in pancreatic cancer is mediated by O-GlcNAc modification of transcription factor Sp1. J Biol Chem **288:** 33927–33938

Birtic S, Ksas B, Genty B, Mueller MJ, Triantaphylidès C, Havaux M (2011) Using spontaneous photon emission to image lipid oxidation patterns in plant tissues. Plant J **67:** 1103–1115

Boca S, Koestler F, Ksas B, Chevalier A, Leymarie J, Fekete A, Mueller MJ, Havaux M (2014) Arabidopsis lipocalins AtCHL and AtTIL have distinct but overlapping functions essential for lipid protection and seed longevity. Plant Cell Environ **37:** 368–381

Bruggeman Q, Raynaud C, Benhamed M, Delarue M (2015) To die or not to die? Lessons from lesion mimic mutants. Front Plant Sci **6:** 24

Caarls L, Pieterse CMJ, Van Wees SCM (2015) How salicylic acid takes transcriptional control over jasmonic acid signaling. Front Plant Sci **6:** 170

Chen S, Dickman MB (2004) Bcl-2 family members localize to tobacco chloroplasts and inhibit programmed cell death induced by chloroplast-targeted herbicides. J Exp Bot **55:** 2617–2623

Clough SJ, Bent AF (1998) Floral dip: A simplified method for *Agrobacterium*-mediated transformation of *Arabidopsis thaliana*. Plant J **16:** 735–743

Danon A, Rotari VI, Gordon A, Mailhac N, Gallois P (2004) Ultraviolet-C overexposure induces programmed cell death in *Arabidopsis*, which is mediated by caspase-like activities and which can be suppressed by caspase inhibitors, p35 and *Defender against Apoptotic Death*. J Biol Chem **279:** 779–787

Danon A, Miersch O, Felix G, Camp RG, Apel K (2005) Concurrent activation of cell death-regulating signaling pathways by singlet oxygen in *Arabidopsis thaliana*. Plant J **41:** 68–80

de Souza AJ, Svozil J, Wang J-Z, Ke H, Xiao Y, Gruissem W, Dehesh K (2017) Cracking the interorganellar communication codes. FASEB J**31:** 617.2

Dricu A, Carlberg M, Wang M, Larsson O (1997) Inhibition of N-linked glycosylation using tunicamycin causes cell death in malignant cells: Role of down-regulation of the insulin-like growth factor 1 receptor in induction of apoptosis. Cancer Res **57:** 543–548

Dubin MJ, Bowler C, Benvenuto G (2008) A modified Gateway cloning strategy for overexpressing tagged proteins in plants. Plant Methods **4:** 3

Fernandez-Bautista N, Dominguez-Nunez JA, Castellano Moreno MM, Berrocal-Lobo M (2016) Plant tissue Trypan Blue staining during phytopathogen infection. Bio Protoc **6:** e2078

Floková K, Tarkowská D, Miersch O, Strnad M, Wasternack C, Novák O (2014) UHPLC-MS/MS based target profiling of stress-induced phytohormones. Phytochemistry **105:** 147–157

Gaffney T, Friedrich L, Vernooij B, Negrotto D, Nye G, Uknes S, Ward E, Kessmann H, Ryals J (1993) Requirement of salicylic acid for the induction of systemic acquired resistance. Science **261:** 754–756

Gallois P, Makishima T, Hecht V, Despres B, Laudié M, Nishimoto T, Cooke R (1997) An *Arabidopsis thaliana* cDNA complementing a hamster apoptosis suppressor mutant. Plant J **11:** 1325–1331

Gan S, Amasino RM (1997) Making sense of senescence Molecular genetic regulation and manipulation of leaf senescence. Plant Physiol **113:** 313–319

Gao C, Xing D, Li L, Zhang L (2008) Implication of reactive oxygen species and mitochondrial dysfunction in the early stages of plant programmed cell death induced by ultraviolet-C overexposure. Planta **227:** 755–767

Ge Y, Cai Y-M, Bonneau L, Rotari V, Danon A, McKenzie EA, McLellan H, Mach L, Gallois P (2016) Inhibition of cathepsin B by caspase-3 inhibitors blocks programmed cell death in Arabidopsis. Cell Death Differ **23:** 1493–1501

Gill SS, Tuteja N (2010) Reactive oxygen species and antioxidant machinery in abiotic stress tolerance in crop plants. Plant Physiol Biochem **48:** 909–930

Goldberg AL (2003) Protein degradation and protection against misfolded or damaged proteins. Nature **426:** 895–899

Gracanin M, Hawkins CL, Pattison DI, Davies MJ (2009) Singlet-oxygen-mediated amino acid and protein oxidation: Formation of tryptophan peroxides and decomposition products. Free Radic Biol Med **47:** 92–102

Greenberg JT (1996) Programmed cell death: A way of life for plants. Proc Natl Acad Sci USA **93:** 12094–12097

Hatsugai N, Yamada K, Goto-Yamada S, Hara-Nishimura I (2015) Vacuolar processing enzyme in plant programmed cell death. Front Plant Sci **6:** 234

Haynes CM, Titus EA, Cooper AA (2004) Degradation of misfolded proteins prevents ER-derived oxidative stress and cell death. Mol Cell **15:** 767–776

He R, Drury GE, Rotari VI, Gordon A, Willer M, Farzaneh T, Woltering EJ, Gallois P (2008) Metacaspase-8 modulates programmed cell death induced by ultraviolet light and H_2O_2 in *Arabidopsis*. J Biol Chem **283:** 774–783

Howden AJM, Salek M, Miguet L, Pullen M, Thomas B, Knight MR, Sweetlove LJ (2011) The phosphoproteome of Arabidopsis plants lacking the oxidative signal-inducible1 (OXI1) protein kinase. New Phytol **190:** 49–56

Jeong IS, Lee S, Bonkhofer F, Tolley J, Fukudome A, Nagashima Y, May K, Rips S, Lee SY, Gallois P, et al (2018) Purification and characterization of *Arabidopsis thaliana* oligosaccharyltransferase complexes from the native host: A protein super-expression system for structural studies. Plant J **94:** 131–145

Kabbage M, Kessens R, Bartholomay LC, Williams B (2017) The life and death of a plant cell. Annu Rev Plant Biol **68:** 375–404

Kawai-Yamada M, Ohori Y, Uchimiya H (2004) Dissection of Arabidopsis Bax inhibitor-1 suppressing Bax-, hydrogen peroxide-, and salicylic acid-induced cell death. Plant Cell **16:** 21–32

Khanna-Chopra R, Nutan KK, Pareek A (2013) Regulation of leaf senescence: Role of reactive oxygen species. *In* Plastid Development in Leaves during Growth and Senescence, B Biswal, K Krupinska, UC Biswal, eds. Springer Netherlands, Dordrecht, pp 393–416

Kim C, Meskauskiene R, Zhang S, Lee KP, Lakshmanan Ashok M, Blajecka K, Herrfurth C, Feussner I, Apel K (2012) Chloroplasts of Arabidopsis are the source and a primary target of a plant-specific programmed cell death signaling pathway. Plant Cell **24:** 3026–3039

Laloi C, Havaux M (2015) Key players of singlet oxygen-induced cell death in plants. Front Plant Sci **6:** 39

Lawton K, Weymann K, Friedrich L, Vernooij B, Uknes S, Ryals J (1995) Systemic acquired resistance in Arabidopsis requires salicylic acid but not ethylene. Mol Plant Microbe Interact **8:** 863–870

Lee HY, Back K (2017) Melatonin is required for H_2O_2- and NO-mediated defense signaling through MAPKKK3 and OXI1 in *Arabidopsis thaliana*. J Pineal Res **62:** e12379

Leister D (2019) Piecing the puzzle together: The central role of reactive oxygen species and redox hubs in chloroplast retrograde signaling. Antioxid Redox Signal **30:** 1206–1219

Le Roux C, Del Prete S, Boutet-Mercey S, Perreau F, Balagué C, Roby D, Fagard M, Gaudin V (2014) The hnRNP-Q protein LIF2 participates in the plant immune response. PLOS One **9:** e99343

Li Z, Wakao S, Fischer BB, Niyogi KK (2009) Sensing and responding to excess light. Annu Rev Plant Biol **60:** 239–260

Lohman KN, Gan S, John MC, Amasino RM (1994) Molecular analysis of natural leaf senscence in *Arabidopsis thaliana*. Physiol Plant **92:** 322–328

Makishima T, Nakashima T, Nagata-Kuno K, Fukushima K, Iida H, Sakaguchi M, Ikehara Y, Komiyama S, Nishimoto T (1997) The highly conserved DAD1 protein involved in apoptosis is required for N-linked glycosylation. Genes Cells **2:** 129–141

Makishima T, Yoshimi M, Komiyama S, Hara N, Nishimoto T (2000) A subunit of the mammalian oligosaccharyltransferase, DAD1, interacts with Mcl-1, one of the bcl-2 protein family. J Biochem **128:** 399–405

Meskauskiene R, Nater M, Goslings D, Kessler F, op den Camp R, Apel K (2001) FLU: A negative regulator of chlorophyll biosynthesis in *Arabidopsis thaliana*. Proc Natl Acad Sci USA **98:** 12826–12831

Moharikar S, D'Souza JS, Rao BJ (2007) A homologue of the defender against the apoptotic death gene (*dad1*)in UV-exposed *Chlamydomonas* cells is downregulated with the onset of programmed cell death. J Biosci **32:** 261–270

Montillet J-L, Cacas J-L, Garnier L, Montané M-H, Douki T, Bessoule J-J, Polkowska-Kowalczyk L, Maciejewska U, Agnel J-P, Vial A, et al (2004) The upstream oxylipin profile of *Arabidopsis thaliana*: A tool to scan for oxidative stresses. Plant J **40:** 439–451

Moreau M, Tian M, Klessig DF (2012) Salicylic acid binds NPR3 and NPR4 to regulate NPR1-dependent defense responses. Cell Res **22:** 1631–1633

Müller-Moulé P, Havaux M, Niyogi KK (2003) Zeaxanthin deficiency enhances the high light sensitivity of an ascorbate-deficient mutant of Arabidopsis. Plant Physiol **133:** 748–760

Nagano M, Ihara-Ohori Y, Imai H, Inada N, Fujimoto M, Tsutsumi N, Uchimiya H, Kawai-Yamada M (2009) Functional association of cell death suppressor, Arabidopsis Bax inhibitor-1, with fatty acid 2-hydroxylation through cytochrome b_5. Plant J **58:** 122–134

Noctor G, Mhamdi A, Chaouch S, Han Y, Neukermans J, Marquez-Garcia B, Queval G, Foyer CH (2012) Glutathione in plants: An integrated overview. Plant Cell Environ **35:** 454–484

Noctor G, Lelarge-Trouverie C, Mhamdi A (2015) The metabolomics of oxidative stress. Phytochemistry **112:** 33–53

Oh SA, Lee SY, Chung IK, Lee C-H, Nam HG (1996) A senescence-associated gene of *Arabidopsis thaliana* is distinctively regulated during natural and artificially induced leaf senescence. Plant Mol Biol **30:** 739–754

op den Camp RGL, Przybyla D, Ochsenbein C, Laloi C, Kim C, Danon A, Wagner D, Hideg E, Göbel C, Feussner I, et al (2003). Rapid induction of distinct stress responses after the release of singlet oxygen in Arabidopsis. Plant Cell**15:** 2320–2332

Petrov V, Hille J, Mueller-Roeber B, Gechev TS (2015) ROS-mediated abiotic stress-induced programmed cell death in plants. Front Plant Sci **6:** 69

Qi T, Wang J, Huang H, Liu B, Gao H, Liu Y, Song S, Xie D (2015) Regulation of jasmonate-induced leaf senescence by antagonism between bHLH subgroup IIIe and IIId factors in Arabidopsis. Plant Cell **27:** 1634–1649

Qiang X, Zechmann B, Reitz MU, Kogel K-H, Schäfer P (2012) The mutualistic fungus *Piriformospora indica* colonizes *Arabidopsis* roots by inducing an endoplasmic reticulum stress-triggered caspase-dependent cell death. Plant Cell **24:** 794–809

Rakhit R, Cunningham P, Furtos-Matei A, Dahan S, Qi XF, Crow JP, Cashman NR, Kondejewski LH, Chakrabartty A (2002) Oxidation-induced misfolding and aggregation of superoxide dismutase and its implications for amyotrophic lateral sclerosis. J Biol Chem **277:** 47551–47556

Ramel F, Ksas B, Akkari E, Mialoundama AS, Monnet F, Krieger-Liszkay A, Ravanat J-L, Mueller MJ, Bouvier F, Havaux M (2013a) Light-induced acclimation of the Arabidopsis chlorina1 mutant to singlet oxygen. Plant Cell **25:** 1445–1462

Ramel F, Ksas B, Havaux M (2013b) Jasmonate: A decision maker between cell death and acclimation in the response of plants to singlet oxygen. Plant Signal Behav **8:** e26655

Reis PAB, Fontes EPB (2012) N-rich protein (NRP)-mediated cell death signaling: A new branch of the ER stress response with implications for plant biotechnology. Plant Signal Behav **7:** 628–632

Reis PA, Carpinetti PA, Freitas PP, Santos EG, Camargos LF, Oliveira IH, Silva JC, Carvalho HH, Dal-Bianco M, Soares-Ramos JR, et al (2016) Functional and regulatory conservation of the soybean ER stress-induced DCD/NRP-mediated cell death signaling in plants. BMC Plant Biol **16:** 156

Rentel MC, Lecourieux D, Ouaked F, Usher SL, Petersen L, Okamoto H, Knight H, Peck SC, Grierson CS, Hirt H, et al (2004) OXI1 kinase is necessary for oxidative burst-mediated signalling in Arabidopsis. Nature **427:** 858–861

Salbitani G, Bottone C, Crafagna S (2017) Determination of reduced and total glutathione content in extremophilic microalga *Galdieria phlegrea.* Bio Protoc **7:** e2372

Sano R, Reed JC (2013) ER stress-induced cell death mechanisms. Biochim Biophys Acta **1833:** 3460–3470

Shumbe L, Chevalier A, Legeret B, Taconnat L, Monnet F, Havaux M (2016) Singlet oxygen-induced cell death in Arabidopsis under high-light stress is controlled by OXI1 kinase. Plant Physiol **170:** 1757–1771

Strasser R (2016) Plant protein glycosylation. Glycobiology **26:** 926–939

Van Breusegem F, Dat JF (2006) Reactive oxygen species in plant cell death. Plant Physiol **141:** 384–390

Vellosillo T, Vicente J, Kulasekaran S, Hamberg M, Castresana C (2010) Emerging complexity in reactive oxygen species production and signaling during the response of plants to pathogens. Plant Physiol **154:** 444–448

Vlot AC, Dempsey DA, Klessig DF (2009) Salicylic acid, a multifaceted hormone to combat disease. Annu Rev Phytopathol **47:** 177–206

von Malek B, van der Graaff E, Schneitz K, Keller B (2002) The Arabidopsis male-sterile mutant *dde2-2* is defective in the *ALLENE OXIDE SYNTHASE* gene encoding one of the key enzymes of the jasmonic acid biosynthesis pathway. Planta **216:** 187–192

Wagner D, Przybyla D, op den Camp R, Kim C, Landgraf F, Lee KP, Würsch M, Laloi C, Nater M, Hideg E, et al (2004) The genetic basis of singlet oxygen-induced stress responses of *Arabidopsis thaliana*. Science **306:** 1183–1185

Walley J, Xiao Y, Wang JZ, Baidoo EE, Keasling JD, Shen Z, Briggs SP, Dehesh K (2015) Plastid-produced interorgannellar stress

signal MEcPP potentiates induction of the unfolded protein response in endoplasmic reticulum. Proc Natl Acad Sci USA **112:** 6212–6217

Wang C, Zien CA, Afitlhile M, Welti R, Hildebrand DF, Wang X (2000) Involvement of phospholipase D in wound-induced accumulation of jasmonic acid in arabidopsis. Plant Cell **12:** 2237–2246

Wildermuth MC, Dewdney J, Wu G, Ausubel FM (2001) Isochorismate synthase is required to synthesize salicylic acid for plant defence. Nature **414:** 562–565

Wituszynska W, Karpinski S (2013) Programmed cell death as a response to high light, UV and drought stress in plants. *In* K Vahdati and C Leslie, eds, Abiotic Stress: Plant Responses and Applications in Agriculture. InTechOpen, London, pp 207–246

Yang ZT, Wang MJ, Sun L, Lu SJ, Bi DL, Sun L, Song ZT, Zhang SS, Zhou SF, Liu JX (2014) The membrane-associated transcription factor NAC089 controls ER-stress-induced programmed cell death in plants. PLoS Genet **10:** e1004243

Yoshimi M, Sekiguchi T, Hara N, Nishimoto T (2000) Inhibition of N-linked glycosylation causes apoptosis in hamster BHK21 cells. Biochem Biophys Res Commun **276:** 965–969

Yulug IG, See CG, Fisher EM, Ylug IG (1995) The DAD1 protein, whose defect causes apoptotic cell death, maps to human chromosome 14. Genomics **26:** 433–435

Zhou C, Cai Z, Guo Y, Gan S (2009) An arabidopsis mitogen-activated protein kinase cascade, MKK9-MPK6, plays a role in leaf senescence. Plant Physiol **150:** 167–177